NUMERICAL STUDY OF LAMINAR FILM BOILING BY FINITE DIFFERENCE METHOD

By

N. SAMBASIVA RAO

DEPARTMENT OF MECHANICAL ENGINEERING

INDIAN INSTITUTE OF TECHNOLOGY, KANPUR

JULY, 1981

NUMERICAL STUDY OF LAMINAR FILM BOILING BY FINITE DIFFERENCE METHOD

A Thesis Submitted
in Partial Fulfilment of the Requirements
for the Degree of
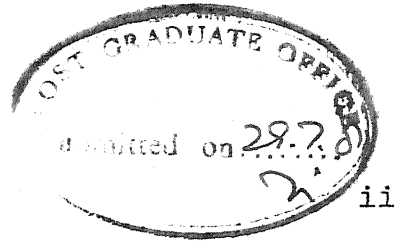
MASTER OF TECHNOLOGY

By
N. SAMBASIVA RAO

to the

DEPARTMENT OF MECHANICAL ENGINEERING

INDIAN INSTITUTE OF TECHNOLOGY, KANPUR

JULY, 1981

TL
621.4022
R18 n

ME-1981-M-RAO-NUM

CERTIFICATE

This is to certify that the thesis entitled, 'Numerical Study of Laminar Film Boiling by Finite-Difference Method' by Mr. N. Sambasiva Rao is a record of work carried out under my supervision and has not been submitted elsewhere for a degree.

(J. Srinivasan)
Assistant Professor
Department of Mechanical Engineering,
Indian Institute of Technology, Kanpur
India

July, 1981

ACKNOWLEDGEMENTS

CONTENTS

LIST OF FIGURES

NOMENCLATURE

T	temperature
ΔT_L	degree of subcooling $= T_{Ls} - T_{L,\infty}$
x	streamwise coordinate
y	cross-stream coordinate
ρ	density
U	velocity in x-direction
V	velocity in y-direction
g	gravitational acceleration
μ	dynamic viscosity
C_p	specific heat
K	thermal conductivity
M_{int}	mass flux density
δ	boundary layer thickness
h_{fg}	latent heat of vapour
ε_w	emissivity of the wall
σ	Stephan-Boltzman constant
t	time
L	length of the plate
U_c	convection velocity
ν	kinematic viscosity
α	thermal diffusivity
Ja	Jacob number
Pe	Peclet number

L	liquid boundary layer thickness
FDE	finite difference equation
η	dimensionless variable = y/δ

Subscripts

w	wall
v	vapour
L	liquid
vs	(property of) vapour at saturation temperature
Ls	(property of) liquid at saturation temperature
∞	at infinity
int	interface
i	suffix used to denote streamwise grid location
j	suffix used to denote cross-stream grid location

ABSTRACT

A numerical study of laminar film boiling by finite-difference method has been carried out. The finite-difference form of the basic conservation equations and interface conditions are solved by the false-transient method. The effect of radiation and the variation of thermophysical properties with temperature are considered in detail. Ratification of the present work is done by comparison with earlier studies. Velocity, temperature, vapour layer thickness and average Nusselt numbers are obtained for water at a pressure of one bar for various degrees of superheating and subcooling. The effect of radiation on vapour layer thickness and total heat transfer rate are illustrated. These results are also compared with experimental data on saturated and subcooled film boiling available in the literature.

CHAPTER I

INTRODUCTION

1.1 Film Boiling:

The name, film boiling, has been given to that type of
boiling which occurs when a complete vapour film exists between
the heated surface and the boiling liquid. Heat exchange
processes accompanied by film boiling are wide spread in such
fields of technology as metallurgy, during thermal treatment
of metals; radio electronics, in temperature control of
electronic equipment, and power production etc. Also, recent
safety measures on nuclear reactors stipulate that the condition
of film boiling should thoroughly be investigated.

During the quenching of materials, a very high tempe-
rature material is suspended inside a liquid. During the
initial period a complex vapour film exists and the cooling of
material is by film boiling heat transfer. The rate at which
the material is cooled initially is important in determining
its structure and hence the film boiling plays a vital role
there.

In radio-electronics film boiling becomes important
in temperature control of electronic equipment. In cryogenic
engineering we come across liquids of very low boiling point.

Film boiling becomes important if the cryogenic liquids
come across surfaces of moderate temperatures. Operation of
jets or rockets frequently involves the contact of a boiling
liquid with hot surfaces.

1.2 Variation of Thermophysical Properties with Temperature
    and Pressure:

In film boiling the temperature difference across the
vapour film is inevitably so large that the temperature dependenc
of properties in the vapour film is severe. This situation
may be easily understood if one thinks about large temperature
difference between the saturated liquid and the surface and
the general steep temperature variation of properties of water
vapour in the proximity of saturation temperature. Also, the
properties vary with pressure and if the system is under pres-
sure, the heat transfer results might be severely affected
by the variation of properties.

The properties that are normally used for calculation
of heat transfer are calculated either at saturation tempera-
ture or at some mean temperature between the wall and the
saturation temperature. Evidently, properties calculated at
saturation temperature will give much error because of large
temperature difference between the wall and saturation tem-
perature. This can be easily seen because the properties at
the wall temperature may be more than twice as large or small
than the properties at the saturation temperature. The

properties calculated at the film temperature may be fair enough if all the properties vary linearly with temperature and the temperature profile is linear inside the vapour-layer. But the density of vapour-varies inversely with absolute temperature (at low pressures) and other properties vary according to some power-law and hence the calculation using the properties at the film temperature will also be in error. The properties vary nonlinearly with pressure and hence if the system is under pressure the constant property model will be in error.

1.3 Effect of Radiation:

Under the film boiling conditions, the rate of heat transfer from a heated surface to a boiling liquid is affected by both convective - conductive transport and by radiative transport. The radiative heat transfer becomes increasingly more important as the surface temperature increases relative to the bulk liquid temperature.

There are two processes by which the radiative transport may affect the film boiling heat transfer. The first is a direct transfer between the heated surface and the liquid. The second is the absorption and emission of radiation in the vapour film which lies between the surface and the liquid. In some cases the vapour may have no absorption or emission bands which lie in the wavelength range of importance to radiative

heat transport. Correspondingly the only radiation effect
is the direct transfer from the surface to liquid. Typical
non-participating gases are Oxygen, Hydrogen, Nitrogen and so
forth. Many vapours including steam have absorption and
emission bands in the thermal range. But the vapour-film
thickness is usually very small and we can consider it
optically thin for radiative transport in most cases. This
way, we can neglect the effect of the participating gas in
radiative heat transfer.

1.4 Review of Literature:

Bromley (1950) was the first person to propose a model
for the problem of film boiling in the presence of radiatively
non-participating vapour. He employed a simple model which
neglected inertia forces and superheating within the vapour-
film and additionally assumed a zero longitudinal vapour
velocity at the liquid-vapour interface. Also, the properties
were assumed constant at film temperature. As discussed in
his paper, Bromley attempted to incorporate the effects of
surface to liquid radiation into the energy equation for the
conductive-convective transport. The resulting differential
equation appeared not to be readily solvable. As an alter-
native he used qualitative arguments to derive a heat transfer
coefficient for the combined convection and radiation process.

P.W. McFadden and R.J. Grosh (1961) analysed the problem of film boiling as a boundary layer problem considering the vapour as a compressible fluid. Only the variations of density and specific heat were considered with temperature and pressure. Other properties were taken constant at film temperature. Also, zero-interface velocity was assumed and radiation was not dealt with.

Later J.C.Y. Koh (1962) made an analysis of the problem in which the shear stress and vapour-velocity at the vapour-liquid interface were taken into account, neglecting the variation of properties and radiation part. Sparrow and Cess (1962) formulated the problem within the frame work of boundary-layer theory in the presence of subcooled liquids, with longitudinal velocity at the vapour - liquid interface assumed as zero.

A thorough investigation with regard to radiation was made by Sparrow in 1964. Consideration was given both to the direct radiation between the heated surface and the liquid and to the emission and absorption of radiation in the vapour layer. He found that the direct surface-to-liquid radiation can appreciably increase the film boiling heat transfer. A quantitative criterion was deduced which states the conditions under which the effects of surface-to-liquid radiation are significant. The results of his analysis (with radiatively participating gas) indicated that the effects of a radiatively

participating vapour on heat-transfer were negligible. In his analysis he assumed zero longitudinal-velocity at the vapour-liquid inter face.

K. Nishikawa and T.Ito (1966) solved this problem in the presence of subcooled liquids in which shear stress and longitudinal velocity at the interface were taken into account. In their analysis, properties were assumed constant and radiation was neglected.

Recently, Nishikawa et.al. (1976) have investigated the variable thermophysical property problem and have showed that the constant property problem gives results which differ widely from that of variable property problem for large temperature differences between the wall to liquid and for higher pressures. Radiative energy transfer was neglected in the analysis.

Sabhapathy (1980) studied the variable property problem with radiation using finite difference method. This is the first known study of film boiling, in which the governing partial differential equations were solved using finite difference techniques. His analysis can be improved significantly because of the following reasons. In that analysis, some significant terms which arose due to the transformation of coordinates (See Sec. 2.4 and Appendix A in this work) were neglected. More importantly , , the convergence criterion he adopted was

not reliable, when the time steps were very small (See Sec.3.1 in this work). Also, he employed the false-transient technique to solve the governing time-dependent partial differential equations, except the equation governing the boundary layer thickness. He solved the last equation using marching techniques. With this approach, however, he was forced to fix the boundary layer thickness at the first streamwise location to control the instabilities.

1.5 Introduction to the Present Work:

In the present work, the effect of property variation and radiation on film boiling are considered together. The finite difference form of the basic conservation equations and interface conditions are solved by the false-transient method. The effect of radiation on heat transfer coefficient is clearly brought-out. Heat transfer coefficient is calculated for various degrees of superheating and subcooling. The accuracy of the present method is checked by comparison with results of Nishikawa et.al. (1976) for the case of no radiation. The results are also compared with experimental data on saturated and subcooled laminar film boiling available in the literature.

CHAPTER II

ANALYSIS

In this chapter, the finite difference form of the basic conservation equations in laminar film boiling from a vertical plate are developed. The symbols used for various parameters and subscripts are indicated under nomenclature.

2.1 Physical Model:

The physical model and the coordinate system for the plane vertical heated plate are shown in Fig. (2.1). The heated plate whose surface is kept at a uniform temperature T_w is submerged vertically in a stagnant boiling liquid whose temperature is lower than the saturation temperature T_{vs} by the degree of subcooling ΔT_L.

Important assumptions made for the derivation of the fundamental equations of conservation laws are; (1) the vapour – liquid interface is smooth and held at saturation temperature, (2) Boundary – layer approximations are valid in the vapour film surrounding the heated plate and the liquid adjacent to it, (3) vapour is assumed to be a non-participating gas while considering the radiative energy transfer from the wall to the interface.

2.2 Governing Equations and Boundary Conditions:

By the physical model and the coordinates described above the fundamental equations for laminar film boiling for vapour and liquid boundary layers are given as follows.

$$\frac{\partial}{\partial x} (\rho_v U_v) + \frac{\partial}{\partial y} (\rho_v V_v) = 0 \tag{2.1}$$

$$\rho_v U_v \frac{\partial U_v}{\partial x} + \rho_v V_v \frac{\partial U_v}{\partial y} = g(\rho_{L,\infty} - \rho_v) + \frac{\partial}{\partial y} (\mu_v \frac{\partial U_v}{\partial y}) \tag{2.2}$$

$$\rho_v C_{p_v} (U_v \frac{\partial T_v}{\partial x} + V_v \frac{\partial T_v}{\partial y}) = \frac{\partial}{\partial y} (K_v \frac{\partial T_v}{\partial y}) \tag{2.3}$$

$$\frac{\partial}{\partial x} (\rho_L U_L) + \frac{\partial}{\partial y} (\rho_L V_L) = 0 \tag{2.4}$$

$$\rho_L U_L \frac{\partial U_L}{\partial x} + \rho_L V_L \frac{\partial V_L}{\partial y} = g(\rho_{L,\infty} - \rho_L) + \frac{\partial}{\partial y} (\mu_L \frac{\partial U_L}{\partial y}) \tag{2.5}$$

$$\rho_L C_{p_L} (U_L \frac{\partial T_L}{\partial x} + V_L \frac{\partial T_L}{\partial y}) = \frac{\partial}{\partial y} (K_L \frac{\partial T_L}{\partial y}) \tag{2.6}$$

The first three equations correspond to the vapour layer. Equation (2.1) representing the continuity, equation (2.2) representing the momentum conservation, and equation (2.3) representing the energy conservation in the vapour layer.

The last three equations represent the continuity, momentum conservation and energy conservation of the liquid layer respectively.

These equations must be compatible with the following relations at the vapour-liquid interface in steady state.

$$M_{int} \equiv \rho_V \left(V_V - U_V \frac{d\delta}{dx}\right)_{int} = \rho_L \left(V_L - U_L \frac{d\delta}{dx}\right)_{int} \quad (2.7)$$

$$(U_V)_{int} = (U_L)_{int} \quad (2.8)$$

$$\left(\mu_V \frac{\partial U_V}{\partial y}\right)_{int} = \left(\mu_L \frac{\partial U_L}{\partial y}\right)_{int} \quad (2.9)$$

$$\left(-K_V \frac{\partial T_V}{\partial y}\right)_{int} + q_R = \left(-K_L \frac{\partial T_L}{\partial y}\right)_{int} - M_{int} h_{fg} \quad (2.10)$$

where $q_R = \varepsilon_w \sigma(T_w^4 - T_{vs}^4)$ and $(T_V)_{int} = (T_L)_{int} = T_{vs} = T_{Ls}$

$$(2.11)$$

Equation (2.7) represents the conservation of mass at the vapour-liquid interface. The continuity of tangential velocity at the interface is represented by equation (2.8). It is nothing but the no slip condition at the interface. Equation (2.9) represents the matching of shear stress at the interface. Equation (2.10) represents the conservation of energy at the interface. The continuity of temperature is represented by equation (2.11).

Other conventional boundary conditions can be written as,

at $y = 0$ $U_V = V_V = 0$ and $T_V = T_w$ $\qquad\qquad$ (2.12)

as $y \to \infty$ $U_L \to 0$ $\qquad$ and $T_L \to T_\infty$ $\qquad\qquad$ (2.13)

Equation (2.12) represents the no slip condition at the wall and the temperature specification. At large distance from the wall the liquid is undisturbed by the presence of the wall and this is represented by equation (2.13). Energy is transferred

from the wall to the liquid by conduction - convection and radiation. The term q_R represents the radiation heat-transfer term. q_R has been evaluated assuming the wall is not black and its emissivity is ε_w and interface is assumed to be black.

2.3 Selection of Numerical Technique:

This type of problem is usually solved by similarity transformation. In the presence of radiation interaction similarity transformation is not possible. So, the partial differential equations are solved numerically by using finite-difference techniques.

These equations can be solved either by marching technique (since the equations are parabolic in x) or by a time-dependent approach such as the false-transient technique. An early work in which both the steady state and the time-dependent approaches were used was that of Hung and Macagno (Roache, 1976). They found that the time-dependent equations were easier to handle and more stable, a conclusion confirmed by many workers since then. Eventhough the philosophy of the time-dependent approach is attractive, it is natural to ask why should one bother with the transient solution in those cases where the only interest is in the eventual steady state solution. Why not set $\partial w/\partial t = 0$ and just work with the steady flow equations? The conclusion obviously depends on the simplicity of the time-dependent method used. For reasonably

simple time-dependent methods, the flexibility of being able to achieve the transient solution if desired, is also attractive. More important, the time-dependent approach does not presume the existence of a steady state solution, which indeed may not exist. It also gives more physical insight into the nature of the equations. This is important in a two-phase problem which has complexities on account of interaction between liquid and vapour.

An attempt was made by Sabhapathy (1980) to solve these equations by marching technique but he was unable to control the instabilities even with very small mesh sizes. We solved the equations using false-transient technique. Here the unsteady state problem is marched in time till a steady state solution is achieved.

2.4 Selection of Grid System:

There are two ways of introducing grid points into the coordinate system. In the first method as shown in Fig.(2.2.1), the x-y coordinate system can be used. If the numerical solution is sought in this x-y coordinate system then it has one important defect; the coordinate system (Cartesian) will not, in general, conform to the shape of the boundary-layer. As the boundary layer grows, more grid points must be added or be carried from the outset of the problem. Thus the scheme involves testing for the outer edge of boundary layer, at

every downstream step by checking the change in the value of W_{ij} at each cross-stream step; the outer edge being defined by the point where $|(\frac{\partial W}{\partial y})_{i,j}|$ is less than a prescribed tolerance. Such a method is uneconomic of computer storage and time. Also, there are grids of curved shape near the vapour-liquid interface, which need special equations to be written at these points. A better technique is to employ a coordinate system that grows with the boundary layer.

In the second method, as shown in Fig. (2.2.2), instead of using y as the cross-stream coordinate, we could use the normalized distance $\eta = y/\delta$, δ being the vapour boundary layer thickness at any x, such that $\eta = y/\delta = 1$ corresponds to the edge of the vapour boundary layer. In this way, the finite difference grid for $0 \le y/\delta \le 1$ would always fit the boundary layer region and the grid points selected initially, at x = 0, say, would lie within the region of interest for all values of x. As the vapour liquid interface always made to correspond to a grid point there can be no problem of curved grids. In the present work, numerical solution is obtained in x - η coordinate system. The following section deals with the changes in the equations of conservation due to transformation of coordinates from x - y to x - η system and the addition of transient term to proceed with the false transient scheme.

2.5 Governing Equations of the Unsteady State Problem in the x - η Coordinate System:

The basic conservation equations given in the x - y coordinate system in Sec. (2.2) are to be modified in the x - η coordinate system, because η - y/δ is a function of both x and y. The equivalent forms of first and second partial derivatives of a variable in the new (x - η) coordinate system are given in Appendix A. The governing equations of the unsteady state problem that are solved are as follows. For the vapour side,

$$\rho_v \left(\frac{\partial U_v}{\partial t} + U_v \frac{\partial U_v}{\partial x} - U_v \frac{\partial U_v}{\partial \eta} \frac{\eta}{\delta} \frac{d\delta}{dx} + V_v \frac{\partial U_v}{\partial \eta} \frac{1}{\delta} \right)$$

$$= g \left(\rho_{L,\infty} - \rho_v \right) + \frac{1}{\delta} \frac{\partial}{\partial \eta} \left(\frac{\mu_v}{\delta} \frac{\partial U_v}{\partial \eta} \right) \qquad (2.14)$$

$$\rho_v C_{p_v} \left(\frac{\partial T_v}{\partial t} + U_v \frac{\partial T_v}{\partial x} - U_v \frac{\partial T_v}{\partial \eta} \frac{\eta}{\delta} \frac{d\delta}{dx} + V_v \frac{\partial T_v}{\partial \eta} \frac{1}{\delta} \right)$$

$$= \frac{1}{\delta} \frac{\partial}{\partial \eta} \left(\frac{K_v}{\delta} \frac{\partial T_v}{\partial \eta} \right) \qquad (2.15)$$

$$\frac{\partial}{\partial x} \left(\rho_v U_v \right) - \frac{\partial}{\partial \eta} \left(\rho_v U_v \right) \frac{\eta}{\delta} \frac{d\delta}{dx} + \frac{1}{\delta} \frac{\partial}{\partial \eta} \left(\rho_v V_v \right) = 0 \qquad (2.16)$$

For the liquid side:

$$\rho_L \left(\frac{\partial U_L}{\partial t} + U_L \frac{\partial U_L}{\partial x} - U_L \frac{\partial U_L}{\partial \eta} \frac{\eta}{\delta} \frac{d\delta}{dx} + \frac{V_L}{\delta} \frac{\partial U_L}{\partial \eta} \right)$$

$$= g \left(\rho_{L,\infty} - \rho_L \right) + \frac{1}{\delta} \frac{\partial}{\partial \eta} \left(\frac{\mu_L}{\delta} \frac{\partial U_L}{\partial \eta} \right) \qquad (2.17)$$

$$\rho_L \, C_{p_L} \left(\frac{\partial T_L}{\partial t} + U_L \frac{\partial T_L}{\partial x} - U_L \frac{\partial T_L}{\partial \eta} \frac{\eta}{\delta} \frac{d\delta}{dx} + \frac{V_L}{\delta} \frac{\partial T_L}{\partial \eta} \right)$$

$$= \frac{1}{\delta} \frac{\partial}{\partial \eta} \left(\frac{K_L}{\delta} \frac{\partial T_L}{\partial \eta} \right) \tag{2.18}$$

$$\frac{\partial}{\partial x} \left(\rho_L \, U_L \right) - \frac{\partial}{\partial \eta} \left(\rho_L \, U_L \right) \frac{\eta}{\delta} \frac{d\delta}{dx} + \frac{1}{\delta} \frac{\partial}{\partial \eta} \left(\rho_L \, V_L \right) = 0 \tag{2.19}$$

The compatibility conditions at the interface are:

At $\eta = 1$:

$$U_v \big|_{int} = U_L \big|_{int} \tag{2.20}$$

$$\frac{\mu_v}{\delta} \frac{\partial U_v}{\partial \eta} \Big|_{int} = \frac{\mu_L}{\delta} \frac{\partial U_L}{\partial \eta} \Big|_{int} \tag{2.21}$$

The mass conservation equation at the interface can be derived (Appendix B) and is given as follows.

$$\rho_L \left[\frac{d\delta}{dt} + U_L \frac{d\delta}{dx} - V_L \right] = \rho_v \left[\frac{d\delta}{dt} + U_v \frac{d\delta}{dx} - V_v \right] \tag{2.22}$$

Similarly the interface energy equation in unsteady state can be stated as follows (See Appendix B for derivation).

$$\rho_v \frac{d\delta}{dt} = \frac{1}{h_{fg}} \left[q_R - \frac{K_v}{\delta} \frac{\partial T_v}{\partial \eta} + \frac{K_L}{\delta} \frac{\partial T_L}{\partial \eta} \right]$$

$$- \rho_v \, U_v \frac{d\delta}{dx} + \rho_v \, V_v \tag{2.23}$$

$$T_{v_{int}} = T_{L_{int}} = T_{Ls} = T_{vs}$$

$$= \text{Saturation temperature} \tag{2.24}$$

The conventional boundary conditions are:

at $\quad \eta = 0 \quad U_V = V_V = 0 \quad$ and $T_V = T_W \qquad$ (2.25)

as $\quad \eta \to \infty \quad T_L = T_\infty = T_{L,\infty}$ and $U_L = 0 \qquad$ (2.26)

2.6 Dimensionless form of the Equations:

The governing equations were non-dimensionalized and the dimensionless variables are given as follows.

(1) $\quad X' = \dfrac{x}{L} \qquad$ (2) $\delta' = \dfrac{\delta}{L} \qquad$ (3) $t' = \dfrac{t \cdot U_c}{L}$

where U_c is the convection velocity ($= [\{g(\rho_{L,\infty} - \rho_{vs})L\}/\rho_{vs}]^{1/2}$) in vapour region.

(4) $\quad U_V' = \dfrac{U_V}{U_c} \qquad$ (5) $V_V' = \dfrac{V_V}{U_c} \qquad$ (6) $T_V' = \dfrac{T_V - T_{vs}}{T_W - T_{vs}}$

(7) $\quad U_L' = \dfrac{U_L}{U_c} \qquad$ (8) $V_L' = \dfrac{V_L}{U_c} \qquad$ (9) $T_L' = \dfrac{T_L - T_{L,\infty}}{T_{Ls} - T_{L,\infty}}$

(10) $\quad \rho_V' = \dfrac{\rho_V}{\rho_{vs}} \qquad$ (11) $\mu_V' = \dfrac{\mu_V}{\mu_{vs}} \qquad$ (12) $K_V' = \dfrac{K_V}{K_{vs}}$

(13) $\quad C_{p_V}' = \dfrac{C_{p_V}}{C_{p_{vs}}} \qquad$ (14) $\rho_L' = \dfrac{\rho_L}{\rho_{Ls}} \qquad$ (15) $\mu_L' = \dfrac{\mu_L}{\mu_{Ls}}$

(16) $\quad K_L' = \dfrac{K_L}{K_{Ls}} \qquad$ (17) $C_{p_L}' = \dfrac{C_{p_L}}{C_{p_{Ls}}}$

The non-dimensional numbers evolved from this non-dimensionalisation are given as follows.

Grashoff number of vapour $= [\dfrac{g(\rho_{L,\infty} - \rho_{vs})L^3}{\rho_{vs} \cdot \nu_{vs}^2}] = $ GRAV

Jacob number of vapour $= \dfrac{C_{p_{vs}}(T_W - T_{vs})}{h_{fg}}$

Peclet number of vapour $= \dfrac{U_c \cdot L}{\alpha_{vs}}$

Jacob number of liquid $= \dfrac{C_{P_{Ls}} (T_{Ls} - T_{L,\infty})}{h_{fg}}$

Peclet number of liquid $= \dfrac{U_c \cdot L}{\alpha_{Ls}}$

From now on in the dimensionless form of the governing equations primes will be removed for brevity. From these final governing equations the finite difference equations will be developed.

Momentum Equation on Vapour Side:

$$\rho_v \left[\frac{\partial U_v}{\partial t} + U_v \frac{\partial U_v}{\partial x} - U_v \frac{\partial U_v}{\partial \eta} \frac{\eta}{\delta} \frac{d\delta}{dx} + \frac{V_v}{\delta} \frac{\partial U_v}{\partial \eta} \right]$$

$$= \frac{\rho_{L,\infty} - \rho_v \cdot \rho_{vs}}{\rho_{L,\infty} - \rho_{vs}} + \frac{1}{\sqrt{GRAV}} \frac{1}{\delta^2} \frac{\partial}{\partial \eta} \left(\mu_v \frac{\partial U_v}{\partial \eta} \right) \quad (2.27)$$

Energy Equation on Vapour Side:

$$\rho_v C_{p_v} \left(\frac{\partial T_v}{\partial t} + U_v \frac{\partial T_v}{\partial x} - U_v \frac{\partial T_v}{\partial \eta} \frac{\eta}{\delta} \frac{d\delta}{dx} + \frac{V_v}{\delta} \frac{\partial T_v}{\partial \eta} \right)$$

$$= \frac{1}{\delta^2} \frac{1}{Pr_{Ls}} \frac{1}{\sqrt{GRAV}} \frac{\partial}{\partial \eta} \left(K_v \frac{\partial T_v}{\partial \eta} \right) \quad (2.28)$$

Continuity Equation on the Vapour Side:

$$\frac{\partial}{\partial x} (\rho_v U_v) - \frac{\partial}{\partial \eta} (\rho_v U_v) \frac{\eta}{\delta} \frac{d\delta}{dx} + \frac{1}{\delta} \frac{\partial}{\partial \eta} (\rho_v V_v) = 0 \quad (2.29)$$

Liquid Side Governing Equations:

Momentum Equation:

$$\rho_L \left(\frac{\partial U_L}{\partial t} + U_L \frac{\partial U_L}{\partial x} - U_L \frac{\partial U_L}{\partial \eta} \frac{\eta}{\delta} \frac{d\delta}{dx} + \frac{V_L}{\delta} \frac{\partial U_L}{\partial \eta} \right)$$

$$= \frac{g \cdot L (\rho_{L,\infty} - \rho_L \cdot \rho_{Ls})}{U_c^2 \cdot \rho_{Ls} \cdot \rho_L} + \frac{\nu_{Ls}}{\rho_L \cdot U_c \cdot L \cdot \delta^2} \frac{\partial}{\partial \eta} (\mu_L \frac{\partial U_L}{\partial \eta})$$

$$(2.30)$$

Energy Equation:

$$\rho_L C_{p_L} \left(\frac{\partial T_L}{\partial t} + U_L \frac{\partial T_L}{\partial x} - U_L \frac{\partial T_L}{\partial \eta} \frac{\eta}{\delta} \frac{d\delta}{dx} + \frac{V_L}{\delta} \frac{\partial T_L}{\partial \eta} \right)$$

$$= \frac{\alpha_{Ls}}{\delta^2} \frac{1}{U_c \cdot L} \frac{\partial}{\partial \eta} (K_L \frac{\partial T_L}{\partial \eta}) \qquad (2.31)$$

Continuity Equation:

$$\frac{\partial}{\partial x} (\rho_L U_L) - \frac{\partial}{\partial \eta} (\rho_L U_L) \frac{\eta}{\delta} \frac{d\delta}{dx} + \frac{1}{\delta} \frac{\partial}{\partial \eta} (\rho_L V_L) = 0 \qquad (2.32)$$

The compatibility conditions at the interface are:

$$\text{at} \quad \eta = 1 \qquad U_v|_{int} = U_L|_{int} \qquad\qquad (2.33)$$

$$\frac{\mu_v \cdot \mu_{vs}}{\delta} \frac{\partial U_v}{\partial \eta} = \frac{\mu_L \cdot \mu_{Ls}}{\delta} \frac{\partial V_L}{\partial \eta} \qquad (2.34)$$

Mass Conservation at the Interface:

$$\rho_L \cdot \rho_{Ls} \left(\frac{d\delta}{dt} + U_L \frac{d\delta}{dx} - V_L \right) = \rho_v \cdot \rho_{vs} \left(\frac{d\delta}{dt} + U_v \frac{d\delta}{dx} - V_v \right)$$

$$(2.35)$$

Interface Energy Balance Equation:

$$\frac{d\delta}{dt} = \frac{\sigma(T_w^4 - T_{vs}^4)}{h_{fg} \cdot \rho_{vs} \cdot U_c} - \frac{Ja_v}{Pe_v} \frac{K_v}{\delta} \frac{\partial T_v}{\partial \eta} + \frac{Ja_L}{Pe_L} \frac{1}{\delta} K_L \frac{\partial T_L}{\partial \eta} \frac{\rho_{Ls}}{\rho_{vs}}$$

$$- \rho_v \left(U_v \frac{d\delta}{dx} - V_v\right) \qquad (2.36)$$

2.7 Numerical Details and Method of Solution:

The length of the plate over which the numerical solution obtained is 0.015 m, because flow is generally not laminar above this height. Although this may seem like an unrealistically small height, the results obtained here can be compared with experimental results on film boiling from thin wires (< 10 mm dia.) where the curvature effects can be neglected. Thus, the number of grid points K chosen along the x-direction determines the space step in the x-direction (= 0.015/K). In the present work K was chosen to be 15.

The number of grid points N, chosen along cross-stream direction in the vapour boundary layer was 10, the N-th grid point corresponding to the vapour-liquid interface. I = 0 corresponds to x = 0, J = 0 corresponds to the wall and M corresponds to the liquid at ∞.

The liquid boundary layer is a conventional boundary layer, its thickness can be defined by arbitrarily defining the edge of the same. The number of grid points was chosen to be 30 (= M - N). This was found to be sufficient

and was also verified from the analytical work of Frederking et.al. (1964). 'See Fig. 2.5.

Method of Solution:

The momentum equation and the energy equation, given above for both gas and liquid, are parabolic in time, contain two independent space coordinates and are coupled through the buoyancy term. These equations along with the continuity equation and the interface compatibility conditions are solved, with the corresponding boundary conditions and initial conditions, by finite difference techniques, employing an explicit, two level method. It is explicit because all the quantities needed to calculate values at the new time step by the finite difference equations are known. It is two-time level because only two-time levels are involved in the calculation.

The partial derivatives in partial differential equations are approximated by suitable finite difference expressions (central difference scheme for diffusion terms and upwind difference scheme for convection terms). This procedure leads to a set of algebraic equations from which the solution for the present time step can be obtained.

By making the grid spacings sufficiently small, the solution obtained by this procedure, is a sufficiently close approximation to the exact solution, if the scheme is convergent, stable and consistent.

The sequence for advancement from an old time level t to a new time level t + Δt is given as follows.

(1)   Velocity (U_V) is calculated in the vapour region for J = 1 to N – 1 from the finite difference form of the vapour momentum equation (2.27).

(2)   Velocity (U_L) is calculated in the liquid region for J = N+1 to M–1 from the finite difference form of the liquid momentum equation (2.30).

(3)   Velocity ($U_{V_{int}} = U_{L_{int}}$) is calculated from the finite difference form of interface shear stress condition (2.34).

(4)   Temperature (T_V) is calculated in the vapour region for J = 1 to N – 1 from the finite-difference form of energy equation (2.28).

(5)   Temperature (T_L) in the liquid is calculated in the liquid region for J = N+1 to M–1 from the finite difference form of the energy equation (2.31).

(6)   Velocity (V_V) is calculated in the. vapour region for J = 1 to N from vapour continuity equation (2.29).

(7)   Boundary-layer thickness (δ) is calculated from the finite difference form of the interface energy conservation equation (2.36).

(8)   Velocity ($V_{L_{int}}$) is calculated from the finite difference form of the interface mass conservation equation (2.42).

(9)   Velocity (V_L) is calculated in the liquid region from the finite difference form of liquid continuity equation (2.39).

Finite Difference Equations:

FDE's were developed by difference approximation to the partial derivatives of the governing equations. These FDE's were used to find variables like velocities, temperatures and the vapour boundary layer thickness.

Finite Difference Approximation to Calculate the Velocity (U_v) from the Equation (2.27) for $J = 1$, N-1:

$$U_{v_{i,j}}^{NEW} = U_{v_{i,j}}^{OLD} + \Delta t \left[- U_{v_{i,j}} \frac{(U_{v_{i,j}} - U_{v_{i-1,j}})}{\Delta x} \right.$$

$$+ U_{v_{i,j}} \frac{(U_{v_{i,j+1}} - U_{v_{i,j}})}{\Delta \eta} \frac{\eta}{\delta_i} \frac{\delta_i - \delta_{i-1}}{\Delta x}$$

$$- \frac{V_{v_{i,j}}}{\delta_i} \frac{(U_{v_{i,j+1}} - U_{v_{i,j}})}{\Delta \eta} + \frac{(\rho_{L,\infty} - \rho_{v_{i,j}} \cdot \rho_{vs})}{(\rho_{L,\infty} - \rho_{vs}) \rho_{v_{i,j}}}$$

$$+ \frac{\mu_{v_{i,j+1}} (U_{v_{i,j+1}} - U_{v_{i,j}}) - \mu_{v_{i,j}} (U_{v_{i,j}} - U_{v_{i,j-1}})}{(\delta_i)^2 \cdot (\Delta \eta)^2 \cdot \sqrt{GRAV}} \right]$$

$$(2.37)$$

Finite Difference Approximation to Calculate the Velocity (U_L) from the equation (2.30) for $J = N+1$ to M-1. (Note: In the terms appearing with * 's index j is to be replaced by $j-1$ if the velocity V_L is positive at that location-upwind scheme).

$$U_{L_{i,j}}^{NEW} = U_{L_{i,j}}^{OLD} + \Delta t \left[-U_{L_{i,j}} \frac{(U_{L_{i,j}} - U_{L_{i-1,j}})}{\Delta x} \right.$$

$$+ U_{L_{i,j}} \frac{(U_{L_{i,j+1}}^* - U_{L_{i,j}}^*)}{\Delta \eta} \frac{\eta}{\delta_i} \frac{\delta_i - \delta_{i-1}}{\Delta x}$$

$$- \frac{V_{L_{i,j}}}{\delta_i} \frac{(U^*_{L_{i,j+1}} - U^*_{L_{i,j}})}{\Delta\eta} + \frac{(\rho_{L,\infty} - \rho_{Ls} \cdot \rho_{L_{i,j}}) \, g \cdot L}{\rho_{Ls} \cdot \rho_{L_{i,j}} \cdot U_c^2}$$

$$+ \nu_{Ls} \frac{\mu_{L_{i,j+1}} (U_{L_{i,j+1}} - U_{L_{i,j}})}{\rho_{L_{i,j}} \cdot (\delta_i)^2 \cdot U_c \cdot L \cdot (\Delta\eta)^2}$$

$$- \nu_{Ls} \frac{\mu_{L_{i,j}} (U_{L_{i,j}} - U_{L_{i,j-1}})}{\rho_{L_{i,j}} \cdot (\delta_i)^2 \cdot U_c \cdot L \cdot (\Delta\eta)^2} \qquad (2.38)$$

Finite difference approximation to calculate the interface tangential velocity $(U_v = U_L)$ from the equation (2.34).

$$U_{v_{i,N}} = U_{L_{i,N}} = \left(\frac{\mu_{vs}}{\mu_{vs} + \mu_{Ls}} \right) U_{v_{i,N-1}}$$

$$+ \left(\frac{\mu_{Ls}}{\mu_{Ls} + \mu_{vs}} \right) U_{L_{i,N+1}} \qquad (2.39)$$

Finite difference approximation to calculate the temperature (T_v) from the equation (2.38) for $J = 1$ to $N-1$:

$$T^{NEW}_{v_{i,j}} = T^{OLD}_{v_{i,j}} + \Delta t \left[- U_{v_{i,j}} \frac{(T_{v_{i,j}} - T_{v_{i-1,j}})}{\Delta x} \right.$$

$$+ U_{v_{i,j}} \frac{(T_{v_{i,j+1}} - T_{v_{i,j}})}{\Delta\eta} \frac{\eta}{\delta_i} \frac{\delta_i - \delta_{i-1}}{\Delta x}$$

$$- \frac{V_{v_{i,j}}}{\delta_i} \frac{(T_{v_{i,j+1}} - T_{v_{i,j}})}{\Delta\eta}$$

$$\left. + \frac{K_{v_{i,j+1}} (T_{v_{i,j+1}} - T_{v_{i,j}}) - K_{v_{i,j}} (T_{v_{i,j}} - T_{v_{i,j-1}})}{Pr_v \cdot \sqrt{GRAV} \cdot (\delta_i)^2 \cdot (\Delta\eta)^2 \cdot \rho_{v_{i,j}} \cdot C_{p_{v,i,j}}} \right]$$

$$(2.40)$$

Finite difference approximation to calculate the temperature (T_L) from the equation (2.31) for $J = N+1$ to $M-1$ (Note: In terms appearing with *'s replace j by j-1 if V_L is positive).

$$T_{L_{i,j}}^{NEW} = T_{L_{i,j}}^{OLD} + \Delta t \left[- U_{L_{i,j}} \frac{(T_{L_{i,j}} - T_{L_{i-1,j}})}{\Delta x} \right.$$

$$+ U_{L_{i,j}} \frac{(T_{L_{i,j+1}}^{*} - T_{L_{i,j}}^{*})}{\Delta \eta} \frac{\eta}{\delta_i} \frac{\delta_i - \delta_{i-1}}{\Delta x}$$

$$- \frac{V_{L_{i,j}}}{\delta_i} \frac{(T_{L_{i,j+1}}^{*} - T_{L_{i,j}}^{*})}{\Delta \eta}$$

$$\left. + \frac{K_{L_{i,j+1}}(T_{L_{i,j+1}} - T_{L_{i,j}}) - K_{L_{i,j}}(T_{L_{i,j}} - T_{L_{i,j-1}})}{\alpha_{Ls} \cdot U_c \cdot L \cdot (\delta_i)^2 \cdot (\Delta \eta)^2 \cdot \rho_{L_{i,j}} \cdot C_{p_{L,i,j}}} \right]$$

$$(2.41)$$

Finite difference approximation to calculate the velocity (V_v) from the equation (2.29) for $j = 1$ to N:

$$V_{v_{i,j}} = \frac{\rho_{v_{i,j-1}} V_{v_{i,j-1}}}{\rho_{v_{i,j}}}$$

$$- \frac{\delta_i \cdot \Delta \eta [(\rho_{v_{i,j}} U_{v_{i,j}} - \rho_{v_{i-1,j}} U_{v_{i-1,j}})/\Delta x]}{\rho_{v_{i,j}}}$$

$$(2.42)$$

Finite difference approximation to calculate the boundary layer thickness (δ) from the equation (2.36).

$$\delta_i^{NEW} = \delta_i^{OLD} + \Delta t \left[\frac{(T_w^4 - T_{vs}^4)}{h_{fg} \cdot \rho_{vs} \cdot U_c} \right.$$

$$- \frac{Ja_v}{Pe_v} \frac{K_{v_{i,N}}}{\delta_i} \cdot \frac{T_{v_{i,N}} - T_{v_{i,N-1}}}{\Delta \eta}$$

$$+ \frac{Ja_L}{Pe_L} \frac{\rho_{Ls}}{\rho_{vs}} \frac{K_{L_{i,N}}}{\delta_i} \frac{T_{L_{i,N+1}} - T_{L_{i,N}}}{\Delta \eta}$$

$$\left. - \rho_{v_{i,N}} (U_{v_{i,N}} \frac{\delta_i - \delta_{i-1}}{\Delta x} - V_{v_{i,N}}) \right] \quad (2.43)$$

Finite difference approximation to calculate the velocity (V_L) at the interface from the equation (2.35):

$$V_{L_{i,N}} = U_{L_{i,N}} \frac{\delta_i - \delta_{i-1}}{\Delta x} + (1 - \frac{\rho_{vs}}{\rho_{Ls}} \frac{\rho_{v_{i,N}}}{\rho_{L_{i,N}}}) \frac{\delta_i^{NEW} - \delta_i^{OLD}}{\Delta t}$$

$$+ \frac{\rho_{vs}}{\rho_{Ls}} \frac{\rho_{v_{i,N}}}{\rho_{L_{i,N}}} (V_{v_{i,N}} - U_{v_{i,N}} \frac{\delta_i - \delta_{i-1}}{\Delta x}) \quad (2.44)$$

Finite difference approximation to calculate the velocity (V_L) in the liquid region from the equation (2.32) for J = N+1 to M-1:

$$V_{L_{i,j}} = \frac{\rho_{L_{i,j-1}} V_{L_{i,j-1}}}{\rho_{L_{i,j}}}$$

$$- \frac{\delta_i \cdot \Delta \eta [(\rho_{L_{i,j}} V_{L_{i,j}} - \rho_{L_{i-1,j}} V_{L_{i-1,j}})/\Delta x]}{\rho_{L_{i,j}}}$$

$$(2.45)$$

It is worth noting that in the above FDE's, all the terms ρ_v, μ_v, K_v, C_{p_v}, ρ_L, μ_L, K_L and C_{p_L} representing thermophysical

properties at any location (I, J) are also dimensionless
variables. Functional variation of these properties with
temperature is given in Appendix C.

The following information might be useful when iterat-
ing the finite difference scheme given above. It was mentioned
earlier that the number of grid points in x-direction was 15.
When the FDE's were iterated at all the 15 grid points, with
the initial conditions, the following observation was made.
All the variables at x - locations nearer to the leading edge
reached steady state in less number of iterations when com-
pared to the variables at far downstream. Variables nearest
to the leading edge reached steady state in smallest number
of iterations. The reason for this can be drawn as follows.

For a variable at any x-location, its domain of
dependence includes a part of upstream region and not down-
stream region, which is a characteristic of parabolic flows.
Since the variables at the leading edge are fixed, the vari-
ables nearest to the leading edge reach steady state in
smallest number of iterations, because significant number of
variables in its domain of dependence were fixed. Based on
this idea, variables at the first x-location (correspond to
I = 1) were iterated till steady state was reached making use
of variables at leading edge (I = 0). After all variables at
I = 1 reached steady state, variables at next x-location (I = 2)

were iterated making use of variables at previous x-location (I = 1). Thus this procedure was repeated upto the last x-location.

The main advantages in this method of solving the problem are

i) Reduction in CPU time, because at each x-location variables converged to steady state in same number of iterations ($\simeq$ 2000).

ii) Computer storage is reduced by a huge amount. In this method of solution only the following variables are to be stored:

a) Variables at the current x-location (say I) at which the variables are being iterated.

b) Variables at the previous x-location (I-1). This way of obtaining the solution reduced the run time charges substantially. The following schematic diagram might help to quickly understand the above mentioned method of solution.

Choice of Initial Profiles:

Vapour velocity in the x-direction (U_v) and the vapour boundary layer thickness (δ) were substituted from Bromley's analysis (1950) at all values of x.

```
        ┌─────────────────────┐
        │ Start with I = 0    │
        │ I represents        │
        │ x-location          │
        └─────────────────────┘
                   │
                   ▼
        ┌─────────────────────┐
───────▶│   I = I + 1         │
        └─────────────────────┘
                   │
                   ▼
        ┌─────────────────┐   Yes   ┌──────┐
        │   If I > 15     ├────────▶│ Stop │
        └─────────────────┘         └──────┘
                   │ No
                   ▼
        ┌─────────────────┐
        │ Set iteration   │
        │ number K = 0    │
        └─────────────────┘
                   │
                   ▼
        ┌─────────────────┐
        │   K = K + 1     │◀──────────┐
        └─────────────────┘           │
                   │                  │
                   ▼                  │
        ┌─────────────────────┐       │
        │ Find new values of  │       │
        │ variables at new    │       │
        │ time level          │       │
        └─────────────────────┘       │
                   │                  │
                   ▼                  │
        ┌──────────────────────────┐  │
  Yes   │ Check for steady state   │  No
◀───────┤ All the variables        ├──┘
        │ reached steady state     │
        │ at location I            │
        └──────────────────────────┘
```

Store the
results in
a file. Now,
you have
have steady
state solu-
tion upto
the latest
value of I
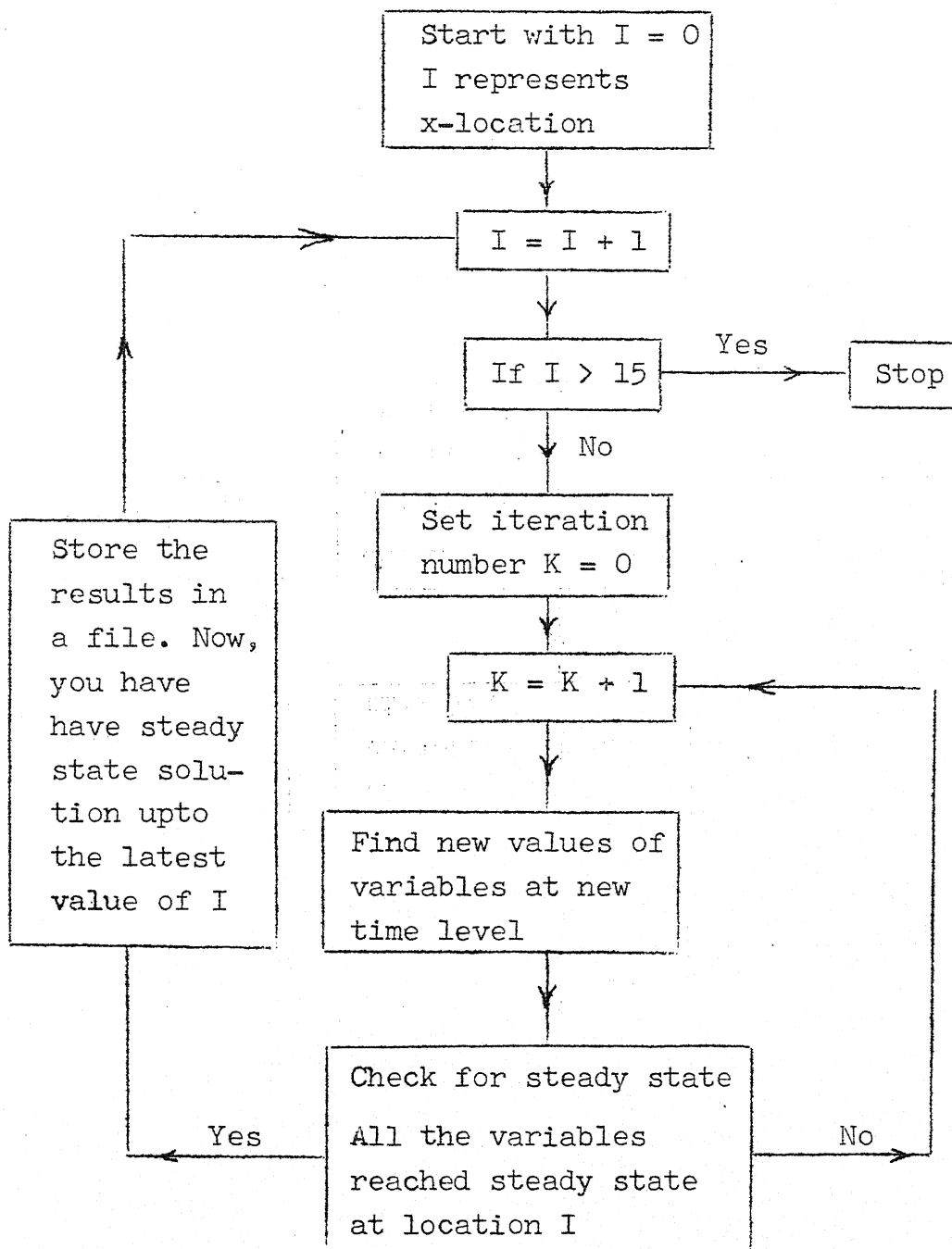
Schematic Diagram

$$\delta = \left[\frac{4 (T_w - T_{vs}) K_{vs} \cdot \mu_{vs} \cdot x}{h_{fg} \cdot g \cdot (\rho_{Ls} - \rho_{vs}) \cdot \rho_{vs}} \right]^{1/4} \qquad (2.46)$$

$$U_v = \frac{(\rho_{Ls} - \rho_{vs}) g \cdot \delta^2 \cdot \eta (2 - \eta)}{2 \mu_{vs}} \quad OR \qquad (2.47)$$

$$U_v = \frac{(\rho_{Ls} - \rho_{vs}) g \cdot \delta^2 \cdot \eta (1 - \eta)}{2 \mu_{vs}} \qquad (2.48)$$

(See Sec. 3.2 for further details about the effect of each of these profiles on stability and convergence of the method)

$$T_v = (T_w - T_{vs}) (1 - \eta) + T_{vs} \qquad (2.49)$$

$$U_L = U_{L,int} (1 - \frac{\delta}{\delta_L} (\eta - 1))^2 \qquad (2.50)$$

$$T_L = (T_{L,int} - T_{L,\infty}) (1 - \frac{\delta(\eta - 1)}{\delta_L})^2 + T_{L,\infty} \qquad (2.51)$$

Vapour velocity in the y-direction was integrated from the continuity equation and the U_v velocity profile (2.47).

$$V_v = \frac{(\rho_{vs} - \rho_{Ls}) \cdot g \cdot \delta^2 \frac{d\delta}{dx} \cdot \eta^2}{2 \mu_{vs}} \qquad (2.52)$$

$$V_L = 0.0 \qquad (2.53)$$

CHAPTER III

NUMERICAL EXPERIMENTS

This chapter is concerned with the difficulties encoun-
tered in obtaining numerical solution to the set of differen-
tial equations presented in the last chapter. The information
about numerical stability and convergence of the scheme can
not be easily understood from theoretical analysis because
of the complicated set of equations with their coupled nature.
The stability and convergence aspects can, however, be studied,
from numerical experiments, the discussion of which is the
subject matter of this chapter. Basic problems of convergence
to a steady state solution and rate of convergence are dis-
cussed at length.

3.1 Convergence Criteria:

The word convergence is used in two different senses,
iteration convergence and truncation convergence. The latter
is well known to us, which has to do with the convergence of
the solution of FDE's to the solution of PDE's as all step
sizes tend to zero. Iteration convergence refers to finally
arriving at a steady state solution of a set of FDE's via
iteration.

There are several problem dependent firm suggestions which we can make about attempting to establish iteration convergence. Out of those, two widely used criteria are discussed here.

a)   Relative error criterion is usually stated as follows:

$$\max_{ij} \left| \frac{W_{ij}^{n+1} - W_{ij}^{n}}{W_{ij}^{n}} \right| \leq \varepsilon \; ; \quad W_{ij}^{n} \neq 0 \qquad (3.1)$$

Here W_{ij}^{n} can be any variable like velocity, temperature or boundary layer thickness at the space point i,j and at time n. This criterion has some weakness in explicit transient methods, when time step is very small. In many transient schemes, time step is governed by stability requirements. If the time step turns out to bevery small, then one has to think of the numerator value in the above criterion (3.1). In such situations, we can take the time step almost equal to zero. Consequently W_{ij}^{n+1} might not be significantly different from W_{ij}^{n} and yet making the whole term on the LHS less than the prescribed value ε, even in very initial stages of iterative scheme. This might certainly lead us to a premature termination. To avoid this, we should constrain ε to take very small values, not greater than 10^{-5} or go for some other criterion.

Thus the above criterion might fail to lead us to steady state in transient schemes when time step is small. When

the question of what is real steady state ? is to be answered, the following criterion might answer in a better way.

b) The other criterion can be stated as follows

$$\max_{ij} \left| \frac{W_{i,j}^{n+1} - W_{i,j}^{n}}{\Delta t} \right| \leq \epsilon \left\{ \begin{array}{l} \text{MOST SIGNIFICANT} \\ \text{term in that} \\ \text{equation} \end{array} \right\} \quad (3.2)$$

In the present work ϵ is taken as 0.01 which was found to be accurate enough. The word MOST SIGNIFICANT is important because, in general all the terms in an equation need not be of the same order of magnitude (ex: convection terms in momentum equation of vapour are very small when compared to viscous and buoyancy terms). Thus comparing transient term with a less significant term in that equation might be a stringent requirement, if not difficult to achieve in practice.

3.2 Choice of Initial Conditions:

To solve the FDE's derived in the last chapter the following initial conditions were used for the saturated film boiling with no radiation.

1) A quadratic velocity profile with no shear stress at the interface was chosen as U velocity profile in the vapour layer.

$$\text{i.e.} \quad U_v \sim \frac{y}{\delta} \left(2 - \frac{y}{\delta} \right)^2 \quad (3.3)$$

2) Linear temperature distribution in vapour layer.

3)   3) V velocity was obtained by integrating the conti-
nuity equation on vapour side.

4)   U velocity on the liquid side was a quadratic profile.

$$U_{Liq} = U_{\substack{vapour\ at \\ interface}} (1 - \frac{y-\delta}{L})^2 \qquad (3.4)$$

5) δ values were obtained from Bromley's analysis (1950).
When FDE's were solved with these initial conditions,
a steady state solution was not reached. The reason for
instability was traced to the choice of zero shear
stress velocity profile in vapour layer. We found that
the evolution of U velocity profiles from the initial
ones was strongly depending upon the choice of initial
velocity profile. Fig. (3.1) shows the possible choices
of initial profiles and their possible directions of
evolution, when the equations were solved with zero-
shear velocity profile, the interface shear condition
satisfied in the way shown in Fig. (3.1a). Also, the
solution was not converging to steady state. Then the
initial U velocity profile was suspected to be an
inappropriate one and Bromley's zero interface velocity
profile was substituted as initial profile,

$$U_{vapour} \sim y/\delta \ (1 - y/\delta) \qquad (3.5)$$

With the above velocity profile, the solution to FDE's
converged to steady state in 22000 iterations (approxi-

mately 20 minutes of CPU time). This is certainly a slow convergence.

3.3 The Effect of Initial Value of Boundary-Layer Thickness:

It was found that the steady state value of δ was very much different from its initial value obtained from Bromley's analysis (See Fig. 3.2). when more refined value of δ was substituted as initial data along with other initial conditions for solving subsequent problems (with varying degrees of superheating and subcooling), a further delay in convergence was observed which can be explained as follows.

The delay in convergence was due to slowly developing (increasing from zero .everywhere) U velocity profile on the liquid side. If large momentum was supplied to the liquid from the interface then the velocity profile might quickly develop to its steady state value. Hence the V velocity in the liquid should be positive. This implies that δ should increase from the initial value because, $d\delta/dt$ represents physically the interface velocity ($\sim$ V velocity of liquid at interface in transient state). But as already mentioned, all variables (including δ), except U velocity in the liquid region, reached steady state after 2000 iterations. It implies that $d\delta/dt$ is almost equal to zero after two thousand iterations. And the only way to make the term ($d\delta/dt$) positive at this stage was to reduce   intentionally from its steady

value. In this way δ was perturbed and convergence was
established in saturated film boiling in 18000 iterations.
Yet this is not a significant achievement. The slow convergence might be due to the use of same non-dimensional timestep in both gas and liquid regions. In fact, the gas region
reached steady state in 2000 iterations and the rest of the
time was taken up by the liquid. This can be explained as
follows.

The time step chosen was because of the stability
requirements on gas side. Also, the allowable time step was
found to be a strong function of the degree of superheating
and subcooling. For decreasing superheating and increasing
subcooling, the allowable time step was found to be decreasing (See Fig. 3.3b). And this could certainly increase the
number of iterations needed for reaching steady state solution
in case of strongly subcooled liquids. But it was noticed
that, as we proceed further seeking solution at downstream
regions, time step can be increased gradually by a significant amount (at least by 4 or 5 times the value of Δt at
leading edge). See Appendix D for a brief explanation. This
can help us in reducing the number of iterations atleast at
downstream regions.

The allowable time steps for varying Δx values, which
can give numerically stable scheme are shown in Fig. (3.3a).
The effect of Δy on time step is very important when compared

to the effect of Δx. The order of magnitude of each effect
on time step is given in Appendix D.

No instabilities were observed on the liquid side
at this time-step (See Appendix D for a brief discussion).
Thus the time step used on the liquid earlier, which was
desired by stability on gas side, was too small for liquid
and it could not come-up to steady state in 2000 iterations.
Based on this, one may conclude that it is desirable to have
two different time steps in order to take advantage of the
higher Δt that can be used in the liquid region. This method
will create difficulties with regard to satisfaction of
interface conditions. The other possibility is to decouple
gas and liquid equations and run them separately and couple
them later. This approach is discussed next.

As the two regions are coupled by the interface condi-
tions, one has to fix a set of values (for velocities) at
the interface, before decoupling can be done. These values
were taken as the values obtained in the last iteration when
both gas and liquid regions were coupled. Thus the two regions
were decoupled and a relatively large time step, approxi-
mately 100 times the allowable time step on the gas side, was
used on the liquid side. Convergence was established on the
liquid side only in 100 iterations, with this large time step.
The advantage of this decoupling is that we can force the slowly

converging liquid region to arrive at steady state solution separately in a small number of iterations. But this steady state on the liquid side may not satisfy the interface conditions. To achieve this, the two regions were coupled for 1000 more iterations and steady state was examined at each and every point. At this stage, all the variables did not satisfy the convergence criterion. Again the liquid region was decoupled and the same procedure was repeated till convergence is established at all points when both gas and liquid regions were coupled. With this approach we arrived at steady state solution in four decouplings (see Schematic diagram 3.4).

A more significant achievement was possible with the use of an over-relaxation technique for the liquid region. The following equation shows the use of relaxation parameter in the liquid momentum equation.

$$U_{ij}^{n+1} = U_{ij}^{n} + \phi \cdot \Delta t \left[\begin{array}{l} \text{contribution due to convection,} \\ \text{buoyancy and diffusion terms} \end{array} \right]$$

$$(3.6)$$

ϕ is the relaxation parameter. When the value ϕ was chosen to be in the range of 100 - 400 (over-relaxation) it was found that the FDE's converged to steady state within 2000 iterations (without any need for decoupling liquid and vapour). This is a major improvement as compared to 18000 - 22,000 iterations required by previous techniques. If a value above 400 is used, then the equations become unstable. With this

```
                         ┌─────────┐
                         │  Start  │
                         └─────────┘
                              │
                              ▼
            ┌──────────────────────────────┐
    ──────▶ │     Iterate the whole        │
            │     region for 2000          │
    ──────▶ │        iterations            │
            └──────────────────────────────┘
                              │
                              ▼
            ┌──────────────────────────────┐
            │  Is steady state estab-      │            ┌────────┐
            │  lished at every point       │   Yes      │  Stop  │
            │  in both gas and liquid      │ ─────────▶ └────────┘
            │         regions?             │
            └──────────────────────────────┘
                              │ No
                              ▼
            ┌──────────────────────────────┐
      No    │  Is only gas region          │
    ◀────── │  reached steady state ?      │
            └──────────────────────────────┘
                              │ Yes
                              ▼
            ┌──────────────────────────────┐
            │ Decouple the liquid region and│
            │ iterate with large time step  │
            │ for a set of interface condi- │
            │ tions till convergence is     │
            │ established.                  │
            └──────────────────────────────┘
                              │
                              ▼
            ┌──────────────────────────────┐
      No    │  Are the interface condi-    │   Yes
    ◀────── │     tions satisfied          │ ──────▶
            └──────────────────────────────┘
```
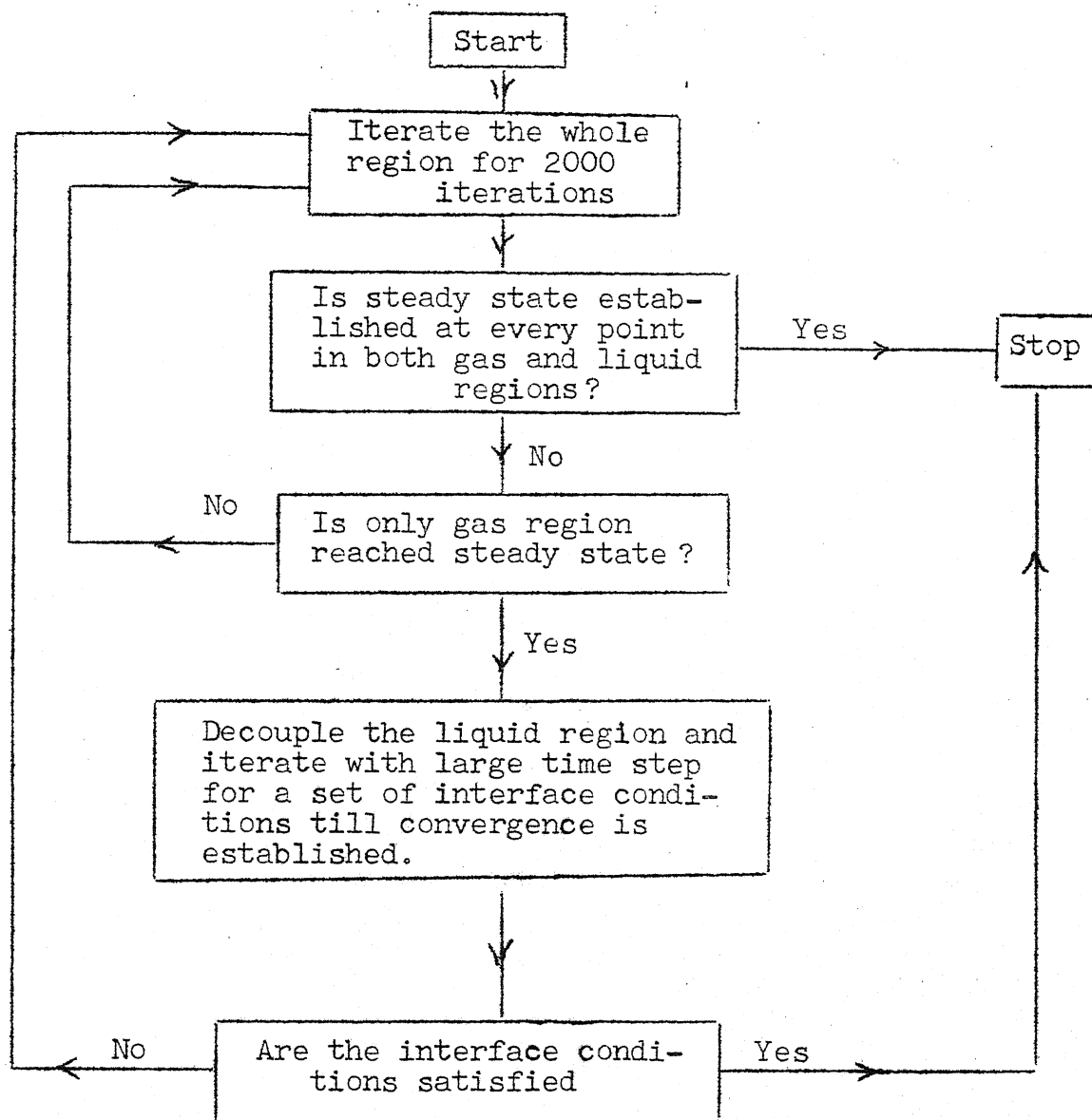
Schematic Diagram 3.4

accelerated convergence the CPU time is 4 minutes for 15 grid points in the x-direction.

3.4 Subcooled Film Boiling:

The numerical solution of conservation equations for the case of subcooled film boiling is somewhat more difficult than that for saturated film boiling because of the presence of energy equation on the liquid side in the former. In the case of subcooled film boiling, the liquid at the interface removes some energy by conduction and convection for heating up the liquid thermal boundary layer. Hence less energy is available for evaporation at the interface. This leads to a reduction in vapour boundary layer thickness. In a numerical scheme, if this reduction occurs rapidly then it can lead to instability as explained below.

Velocity V_y in the liquid at the interface is calculated from mass conservation equation (2.35). Hence, this velocity is dependent on (1) rate of change of boundary layer thickness $(d\delta/dt)$, (2) shape of the vapour boundary layer $(d\delta/dx)$, (3) rate of liquid disappearance because of evaporation. At low pressures the density of liquid is much larger than that of vapour and hence the third term above makes negligible contribution. In the numerical scheme the initial velocity V_y on the liquid side was based on the results of saturated film boiling. If the degree of subcooling is $1^{\circ}K$ then the

finite difference equations converged satisfactorily. In the initial stages, the time step was chosen to be half that of saturated film boiling. At higher degrees of subcooling (around $5^{\circ}K$) the numerical scheme showed tendency to become unstable. This can be explained as follows.

In the initial stages the velocity V_y is determined primarily by the rate of change of vapour boundary-layer thickness with time $(d\delta/dt)$. In the case of $1^{\circ}K$ subcooling the velocity V_y was small (~ 0.3 m/S) because $(d\delta/dt)$ was small. On the other hand in the case of $5^{\circ}K$ subcooling the velocity V_y became very large (~ 1400m/S) and this resulted in instability. When the velocities in the liquid region are very large, the present analysis will not be valid (for instance, boundary layer approximations will not hold good when the cross-stream velocity is comparable to streamwise velocity).

One of the reasons for the large $d\delta/dt$ in higher degrees of subcooling was traced to a significant change in temperature in the liquid. In order to bring only a small change in temperature with time an under relaxation technique was employed to energy equation which was similar to the one described in Secs.3.3 and 3.5, but with a value of $\phi = 0.01$

(under relaxation). But this became not successful. Hence, it was decided to neglect the term $d\delta/dt$ totally in order to eliminate this instability. Nevertheless the set of equations are still quite valid in steady state because $d\delta/dt$ is zero in steady state. This was even verified from the saturated film boiling results. With this modification no further instability was observed and the iterated solution converged to steady state.

3.5 Over-Relaxation Technique:

While solving the FDE's for the case with subcooling an over-relaxation was used which accelerated the convergence on the liquid side. The following equation shows the use of relaxation parameter in the liquid momentum and energy equations.

$$ W_{ij}^{n+1} = W_{ij}^{n} + \phi \; \Delta t \; [A + B + C] $$

where W_{ij}^{n} can be either temperature or velocity on the liquid side, and

A = Contribution due to convection terms
B = Contribution due to diffusion terms
$\left.\right\}$ In momentum and energy equations

C = Contribution due to Buoyancy term in momentum eqn.

  = 0 in energy equation

(See Eqns. 2.30 and 2.31)

The value of ϕ was varied from 100 to 500 (over relaxation) and it was found that for values greater than 400 the scheme was unstable. In the present work its value was taken to be 250. Even though this technique was first developed in solving subcooled film boiling, the technique was also employed in solving FDE's in saturated film boiling for varying degrees of super heating and already mentioned in Sec. 3.3. With this accelerated convergence the iterated solution reached steady state in 2000 iterations with a CPU time of 7.5 minutes for fifteen grid points in the x-direction. Also, it was found that a significant amount of CPU time was taken up by calculation of properties (around 3 minutes of CPU time).

CHAPTER IV

RESULTS AND DISCUSSIONS

The present finite-difference scheme is ratified by comparing heat-transfer coefficient, velocity and temperature profiles (for NO RADIATION CASE), with those obtained by Nishikawa et.al. (1970) who used similarity transformation and solved a set of ordinary differential equations.

In order to examine the effect of variable properties and radiation, the degree of superheating, subcooling are varied for water at 1 bar pressure. All the relevant properties in the governing equations are regarded as temperature-dependent when solutions with variable property are to be obtained, while in calculation with constant property these are evaluated at the saturation or the film temperature (arithmetic mean of the wall and saturation temperature). Solutions are obtained for various degrees of superheating and subcooling, when radiative effects are neglected. By a comparison of the results obtained without radiation to those obtained with radiation, the effect of radiation on heat-transfer coefficient is clearly brought-out.

4.1 Ratification of the Present Work:

. The comparison of the values of $hx^{1/4}$ in Fig. (4.1)
for various degrees of superheating and subcooling indicates
very good agreement with those obtained by Nishikawa et.al.(1976).
The comparison was done with the values of $hx^{1/4}$ because,
Nishikawa et.al. showed that $hx^{1/4}$ has the same value for given
macro-parameters (such as pressure, degree of superheating and
degree of subcooling) and do not depend on the height x. In
Fig. (4.2) velocity and, temperature profiles in the vapour
are compared for a typical degree of superheating (= 449°K
and $\Delta T_L = 40^\circ$K). The comparison indicates a close agreement
near the wall and some disparity away from the wall in both
velocity and temperature profiles in the vapour region. This
disparity away from the wall can partially be attributed to
the error introduced in the transformation of non-linear
abscissa – used by Nishikawa et.al. to a more convenient
η = y/δ abscissa used in the present work (See Appendix E
for further details). The above comparisons indicate that the
present finite difference scheme with grid spacing ($\Delta x = 1$ mm
$\Delta y = 0.1 \delta$) gives acceptable accuracy.

4.2 Discussion on V Velocity in Vapour and Liquid Regions:

In Fig. (4.3), we see the variation of V velocity with
distance away from the wall in both vapour and liquid regions.
As we see in the figure, the velocity is negative all the way

in the vapour region and is maximum near the inter face. A discontinuity in V velocity exists at the inter face which can be explained as follows.

V velocity in liquid region at the interface is found from inter face mass conservation equation (2.35). In steady-state, the V velocity is positive near the inter face as shown in Fig. (4.3). At the first instant, one might be skepti-cal about the validity of this result, because a negative V velocity is required to supply liquid at the inter face. But the fact that even this positive V velocity can supply liquid at the interface is explained based on the curvature of the inter face.   By considering the streamline drawn in Fig.(4.4a), we can conclude the following. (1) Liquid is moving towards interface all the way. Thus, it supplies required mass at the interface. (2) In the coordinate system shown in Fig. (4.4b) velocity of liquid near the interface is positive.

So, this positive V velocity near the interface is a feasible solution. With this, the mass conservation is satis-fied as shown in Fig. (4.4c). Other possible way in which mass conservation can be satisfied is shown in Fig. (4.4d). If this is the way in which mass is conserved, then it says that liquid with its density 1600 times the density of vapour (at low pressures) is entering vapour-layer in BOTH x and y direc-tions ONLY to supply the net amount of vapour leaving that

particular differential element, which might not be physically possible unless the order of vapour velocity (or density) is very high.

Thus, the mass conservation with positive V velocity is seemingly more correct at low pressures. At this juncture, we would like to discuss an important consequence of this new result.

Interface with no curvature (Flat Interface): For this case, $d\delta$ is zero at all x. If liquid is to be supplied at the interface, then V velocity in the liquid region should be negative for this flat interface condition as shown in Fig. (4.4e). For the boundary-layer problem $d\delta/dx$ (one measure of curvature of the interface) varies with x, decreases with increase in x. With increase in x, the curvature of the interface approaches that of the hypothetical flat interface in which case, one can expect more region near the interface on the liquid side with negative V velocity. This important feature was readily observed in the present work. At the leading edge (where $d\delta/dx$ is maximum) in a comparatively large liquid region(5 points away from interface) V velocity is positive and at downstream stations V is positive in a relatively smaller region (only 3 points away from the interface). see Fig. (4.4f). Thus,it shows clearly that we can attribute the positive nature of V velocity near the interface to the curvature of the interface.

4.3 Effect of the Variation of Properties with Temperatures:

In Fig. (4.5), we see the average Nusselt number
(defined in Appendix F) for different degrees of superheating
in saturated film boiling. The results of numerical solution
for variable properties are compared with those for constant
properties. In the case of constant property solution there
are two approaches. One is the evaluation of all properties
at saturation temperature and the other approach is to eva-
luate them at the film temperature. This figure shows that
the evaluation of properties at film temperature is accurate
enough for most applications because, this approach predicts
heat-transfer coefficients very close to those with variable
properties at low pressures.

But it clearly shows that the evaluation of proper-
ties at saturation temperature could not predict the heat-
transfer coefficients accurately even at low pressure (1 bar).
Even though, one might always prefer to evaluate properties
at film temperature (if the mean temperature can be calculated),
evaluation of properties at the saturation temperature is an
alternative to start with when the mean temperature can not be
found out before hand (in case of constant heat flux boundary
condition at the wall). So, this figure infers an important
fact that film temperature criterion is preferable to the
saturation temperature. And the saturation temperature approach
predicts a lower average Nusselt number at least by 35 percent

at higher degrees of superheating when compared with variable
property approach.

In Fig. (4.6), we see the effect of individual property
variation on heat transfer for saturated film boiling. From the
figure it is obvious that the effect of variation of specific
heat is almost negligible at low pressures. All other proper-
ties that are assumed constant are evaluated at saturation
temperature.   Curve 1 shows the effect of variable viscosity.
Its effect is to decrease heat transfer and the average Nusselt
number is in large error at higher degrees of superheating. The
effect of variable density along with variable viscosity is to
further decrease the heat transfer as shown in curve 2. There-
fore, the effect of promotion of heat transfer caused by the
increase of body force due to the reduced density cannot
over come the effect of deterioration of heat-transfer caused
by the increase of thickness of vapour film. Curve 3, in one
way, shows the effect of variation of specific heat and in other
way, shows the effect of variation of thermal conductivity,
Thus, the variation of thermal conductivity, viscosity and
density could alone predict the heat transfer results accura-
tely for engineering analysis.   In other words, we can neglect
the variation of specific heat in solving the variable property
film boiling problem.

4.4 Effect of Radiation on Heat-Transfer Results:

Figure (4.7) shows the effect of radiation on the vapour boundary layer thickness for varying degrees of superheating and subcooling. In Fig. (4.7a) we see the effect of radiation on the vapour-boundary layer thickness for saturated film boiling. Radiation increases the thickness of vapour film everywhere and the effect is seen to be more predominant as the vapour layer thickness increases. This is because, as the vapour layer thickness increases, the convective heat transfer goes down and the radiative heat transfer (which is constant) plays a relatively more important role. The same figure shows that an increase in the degree of superheating increases the effect of radiation on boundary layer thickness which is easy to understand. Fig. (4.7b) shows the effect of radiation in subcooled boiling. It shows that the effect of radiation is small with increasing subcooling and decreasing superheating.

Fig. (4.8) shows the effect of radiation on average Nusselt number (defined in Appendix F) for varying degrees of superheating and subcooling. Many important points can be inferred from this figure. First of all, it can be seen that the effect of radiation is to enhance the total heat transfer. This conclusion is consistent with the results predicted by Sharrow (1964). Without radiation, $Nu_{average}$ decreases with

increase in degree of superheating and increases with increase
in degree of subcooling. It is interesting to note that when
radiation is included, the $Nu_{average}$ increases with degree of
superheating for saturated film boiling. In subcooled film
boiling the effect of radiation is less and the average Nusselt
number decreases initially and increases after some degree of
superheating. This trend is very much supported by experimental
data shown in Figs. (4.9a) and (4.9c).

Radiation affects the heat transfer in the vapour
layer in two ways. Radiation directly increases the heat-
transfer by providing an alternative parallel path. It also
indirectly decreases the heat-transfer by convection by
increasing the thickness of the boundary layer. The combined
effect is to increase the heat transfer as shown in Fig. (4.8).

Thus, even though, $Nu_{average}$ without radiation decreases
all the way with increase in degree of superheating, the inclu-
sion of radiation shows the complicated nature of variation of
$Nu_{average}$ for varying degrees of superheating and subcooling.

An attempt was made to compare the results obtained
from the present work for saturated boiling (with radiation)
with those obtained by Sparrow (1964). Unfortunately, the
length of the plate considered by Sparrow was 10 cm which
is unrealistically high for laminar film boiling. However, the
effect of radiation in terms of the ratio of q/q_o (q is the

local heat transfer with radiation and q_o is the local heat
transfer without radiation) is compared for a typical value of
x ($\sim$ 1.1 cms). Nevertheless, the comparison indicates that
the trend of the effect of radiation on heat transfer is same
in both cases, but the above mentioned ratio turned out to be
1.66 in the present work and sparrow obtained it as 1.92 for
a degree of superheating equal to 800 K. The assumptions made
by Sparrow (Sec. 1.4) might be the main reason for this dis-
parity (See Appendix F for details).

Bromley in his work (1950), suggested a simple method
for including the effect of radiation. The validity of that
criterion is verified with the results obtained in a more
precise manner in this work (See Appendix F for the verifica-
tion of Bromley's rule for accounting radiation). From the
values in the table in Appendix F, it can be concluded that
Bromley s rule for accounting radiation is quite good and
the disparity is not more than three percent.

4.5 Comparison with Available Data:

Comparison between the present numerical results (with
full variable property and with radiation) and the experimental
data (obtained by Nishikawa et al (1976)) is shown in Fig.(4.9).

The details regarding the transformation of flat plate
numerical results to horizontal cylinders are shown in Appen-
dix F.

Experimental data plotted in Fig. (4.9a) are for hori-
zontal cylinder of 13 mm diameter. Theoretical results obtained
by Nishikawa et.al. (1976) are also plotted in the same figure.
As it is clear from the figure, data of saturation film
boiling for cylinder with 13 mm is in good agreement with the
present numerical results with radiation. At the same time,
the theoretical results obtained by Nishikawa et.al.(who
neglected radiation) predicts a smaller average heat-transfer
coefficient. Appendix F contains the quantitative comparison
of both these results with experimental data.

Fig. (4.9b) shows the experimental data for horizon-
tal cylinder of 6 mm diameter. The results obtained in the
present work are in small disagreement with the experimental
data. As the present analysis is done with more sophistication,
the disparity can be attributed to the curvature effect because
of the small diameter of the cylinder, since in this case, the
thickness of the vapour film is comparable to radius of the
cylinder.

Experimental data for subcooled film boiling $(\Delta T_L = 20 \, K)$
are plotted in Fig. (4.9c) for horizontal cylinder of 16 mm
diameter. Even though the results obtained in the present work
are higher than the experimental data they are in better agree-
ment with experimental data when compared to those obtained
by Nishikawa et.al. (1976). More importantly, in the present

analysis, the wall is assumed as a perfect black surface which can hardly be met with real material surfaces. Nishikawa et.al. (1976) did not mention the emissivity of the cylinder surface. The assumption of emissivity equal to 1.0 might be one of the reasons for the over prediction of average heat transfer coefficient when compared to the experimental data. Generally the emissivities of oxidized metallic surfaces are in the range of 0.8 to 0.9.

4.6 Suggestions for Future Work:

The results obtained in the present work are for water at 1 bar pressure. The program listed in Appendix G can be used to obtain results for any liquid at any pressure without any difficulty, if the property variations can be obtained as functions of temperature and pressure in the polynomial form.

Also, the analysis done in the present work is for laminar film boiling. The more commonly encountered turbulent film boiling can be studied with the same program, if good data is obtained on the spatial variation of eddy diffusivity in the vapour and liquid regions.

The analysis made in the present work is for natural convection film boiling and it is yet to be seen and worth trying, if the same program can yield results for a mixed convection film boiling problem. This can be achieved numerically, by imposing a proper velocity (so that it should neither

be biased towards forced convection nor natural convection)
at the far end in the liquid region.

In the present analysis, the vapour lying between the
wall and interface is assumed to be non-participating gas
for radiation. Eventhough Sparrow (1964) showed that the
effect of the participating nature of water vapour is totally
negligible at low pressures, it is worth doing the analysis
again with more reasonable assumptions (because, Sparrow
assumed the vapour to be a gray gas).

REFERENCES

1. Bromley, L.A., Heat transfer in stable film boiling, Chem. Eng. Progr. 46, 221 (1950).

2. P.W. McFadden and R.J. Grosh, An analysis of laminar film boiling with variable properties. Int. J.Heat Mass Transfer 9, 103 (1961).

3. J.C.Y. Koh, Analysis of film boiling on vertical surfaces, J. Heat Transfer 84, 55 (1962).

4. T.N.K. Frederking, Laminar two-phase boundary layers in natural convection film boiling, Z. Angew. Math.Phys. 14, 207 (1963).

5. T.N.K. Frederking and J.Hopenfeld, Laminar two-phase boundary layers in natural convection film boiling of a subcooled liquid. Z.Angew.Math. Phys. 15, 388 (1964).

6. E.M. Sparrow, The effect of radiation on film boiling heat transfer. Int.J. Heat Mass Transfer 7, 229 (1964).

7. K. Nishikawa and T.Ito, Two-phase boundary layer treatment of free convection film boiling, Int. J. Heat Mass Transfer 9, 103 (1966).

8. K. Nishikawa, T.Ito and K. Matsumoto, Investigation of variable thermophysical property problem concerning film boiling from vertical plate with prescribed uniform temperature. Int. J. Heat Mass Transfer 19, 1175 (1976).

9. Roache, J. Patrick, Computational Fluid Dynamics, Revised Edition, Hermosa Publishers, Albuquerque, USA, 1976.

10. P. Sabhapathy, Numerical study of radiative effects in film boiling from a vertical plate, M.Tech. Thesis, IIT Kanpur, 1980.

APPENDIX A

If the original governing equations are in x-y (Cartesian) coordinate system and if, for convenience, the x-y coordinate system is to be transformed to $\xi(x, y)$ - $\eta(x, y)$ coordinate system, then accordingly all the partial derivatives should also be transformed into the new ξ - η coordinate system using the following formulae.

If the original coordinate system is x - y and the new coordinate system is ξ - η , where ξ and η are functions of x and y and w is any dependent variable, then

$$\frac{\partial w}{\partial x} = \frac{\partial w}{\partial \xi} \cdot \frac{\partial \xi}{\partial x} + \frac{\partial w}{\partial \eta} \cdot \frac{\partial \eta}{\partial x} \qquad (A1)$$

$$\frac{\partial w}{\partial y} = \frac{\partial w}{\partial \xi} \cdot \frac{\partial \xi}{\partial y} + \frac{\partial w}{\partial \eta} \cdot \frac{\partial \eta}{\partial y} \qquad (A2)$$

$$\frac{\partial^2 w}{\partial x^2} = \frac{\partial^2 w}{\partial \xi^2} \left(\frac{\partial \xi}{\partial x}\right)^2 + 2 \frac{\partial^2 w}{\partial \xi \partial \eta} \cdot \frac{\partial \xi}{\partial x} \cdot \frac{\partial \eta}{\partial x} + \frac{\partial^2 w}{\partial \eta^2} \cdot \left(\frac{\partial \eta}{\partial x}\right)^2$$

$$\frac{\partial w}{\partial \xi} \cdot \frac{\partial^2 \xi}{\partial x^2} + \frac{\partial \omega}{\partial \eta} \cdot \frac{\partial^2 \eta}{\partial x^2} \qquad (A3)$$

$$\frac{\partial^2 w}{\partial x \partial y} = \frac{\partial^2 w}{\partial \xi^2} \cdot \frac{\partial \xi}{\partial x} \cdot \frac{\partial \xi}{\partial y} + \frac{\partial^2 w}{\partial \xi \partial \eta} \left[\frac{\partial \xi}{\partial x} \cdot \frac{\partial \eta}{\partial y} + \frac{\partial \xi}{\partial y} \cdot \frac{\partial \eta}{\partial x} \right]$$

$$+ \frac{\partial^2 w}{\partial \eta^2} \cdot \frac{\partial \eta}{\partial x} \cdot \frac{\partial \eta}{\partial y} + \frac{\partial w}{\partial \xi} \cdot \frac{\partial^2 \xi}{\partial x \partial y} + \frac{\partial w}{\partial \eta} \cdot \frac{\partial^2 \eta}{\partial x \partial y} \qquad (A4)$$

$$\frac{\partial^2 w}{\partial y^2} = \frac{\partial^2 w}{\partial \xi^2} \left(\frac{\partial \xi}{\partial y}\right)^2 + 2\frac{\partial^2 w}{\partial \xi \partial \eta} \cdot \frac{\partial \xi}{\partial y} \cdot \frac{\partial \eta}{\partial y} + \frac{\partial^2 w}{\partial \eta^2}\left(\frac{\partial \eta}{\partial y}\right)^2$$

$$+ \frac{\partial \omega}{\partial \eta} \cdot \frac{\partial^2 \eta}{\partial y^2} + \frac{\partial w}{\partial \xi} \cdot \frac{\partial^2 \xi}{\partial y^2} \tag{A5}$$

Applying these formulae to the present problem.

Initially it was x-y coordinate system. New coordinate system is x - η

$$\therefore \quad x = x, \quad \eta = \eta(y, \delta) = \eta(y, \delta)$$

$$\therefore \quad \frac{\partial w}{\partial x} = \frac{\partial \delta}{\partial x} \cdot \frac{dx}{dx} + \frac{\partial w}{\partial \eta} \cdot \frac{\partial \eta}{\partial x} = \frac{\partial w}{\partial x} + \frac{\partial w}{\partial \eta} \cdot \frac{\partial}{\partial x}(y/\delta)$$

$$= \frac{\partial w}{\partial x} - \frac{\partial w}{\partial \eta} \cdot \frac{y}{\delta^2} \cdot \frac{d\delta}{dx} = \frac{\partial w}{\partial x} - \frac{\partial w}{\partial \eta} \cdot \frac{\eta}{\delta} \cdot \frac{d\delta}{dx} \tag{A6}$$

$$\frac{\partial w}{\partial y} = \frac{\partial w}{\partial x} \cdot \frac{dx}{dy} + \frac{\partial w}{\partial \eta} \cdot \frac{\partial \eta}{\partial y} = 0 + \frac{\partial w}{\partial \eta} \cdot \frac{\partial}{\partial y}(y/\delta)$$

$$= \frac{1}{\delta} \cdot \frac{\partial w}{\partial \eta} \tag{A7}$$

$$\frac{\partial^2 w}{\partial y^2} = \frac{\partial^2 w}{\partial x^2} \cdot \frac{d^2 x}{dy^2} + 2\frac{\partial^2 w}{\partial x \partial y} \cdot \frac{dx}{dy} \cdot \frac{\partial \eta}{\partial y} + \frac{\partial^2 w}{\partial \eta^2}\left(\frac{\partial \eta}{\partial y}\right)^2$$

$$+ \frac{\partial w}{\partial x} \cdot \frac{d^2 x}{dy^2} + \frac{\partial w}{\partial \eta} \cdot \frac{\partial^2 \eta}{\partial y^2}$$

$$= \frac{\partial^2 w}{\partial \eta^2}\left(\frac{\partial \eta}{\partial y}\right)^2 = \frac{1}{\delta^2} \cdot \frac{\partial^2 w}{\partial \eta^2} \tag{A8}$$

Other partial derivatives are irrelevent to this problem.

APPENDIX B

Mass Conservation at the Interface:

Mass conservation equation in transient state can be derived as follows.

By taking a control volume at the interface as shown in Fig. (2.3) we can write the mass balance as follows:

Mass of vapour and liquid leaving the control volume per unit time

$$= U_v \cdot d\delta - V_v \cdot dx + V_L \, dx - U_L \cdot d\delta \qquad (B1)$$

Change in the mass of vapour and liquid in the control volume per unit time

$$= \rho_L \cdot \frac{d\delta}{dt} \cdot dx - \rho_v \cdot \frac{d\delta}{dt} \cdot dx \qquad (B2)$$

(1) and (2) should be equal for mass conservation

$$\therefore \rho_L \left[\frac{d\delta}{dt} + U_L \cdot \frac{d\delta}{dx} - V_L \right] = \rho_v \left[\frac{d\delta}{dt} + U_v \frac{d\delta}{dx} - V_v \right]$$

$$(B3)$$

Energy Balance at the Interface:

Rate of vapour generation can be found by writing energy balance at the interface.

$$M_{int} = \text{Rate of vapour generation per unit length along the plate} = \frac{1}{h_{fg}} \left[q_R - \frac{K_v}{\delta} \frac{\partial T_v}{\partial n} + \frac{K_L}{\delta} \cdot \frac{\partial T_v}{\partial n} \right]$$

$$(B4)$$

Making use of this, the equation (2.23) which governs the change in boundary-layer thickness with time can be derived as follows. By taking a control volume as shown in Fig.(2.4) we can write the mass balance as follows.

Rate of vapour generation - Net flow rate of vapour

= Rate of change in mass in control volume   (B5)

Now, we shall derive the expression for net flow rate of vapour in a differential vapour boundary layer element. By observing the same fig. (2.4) the net flow rate in x-direction over a differential length dx can be written as

$$= \dot{m}_{x+dx} - \dot{m}_x$$

where,

$$\dot{m}_{x+dx} = \int_0^{\delta+d\delta} \rho_v U_v \big|_{x+dx} \cdot dy \quad \text{and} \quad \dot{m}_x = \int_0^{\delta} \rho_v U_v \big|_x \, dy$$

$$\therefore \quad \dot{m}_{x+dx} - \dot{m}_x = \int_0^{\delta+d\delta} \rho_v U_v \big|_{x+dx} \, dy - \int_0^{\delta} \rho_v U_v \big|_x \, dy$$

$$= \int_0^{\delta+d\delta} \left[\rho_v U_v \big|_x + \frac{\partial}{\partial x}(\rho_v U_v)\cdot dx\big|_x + \ldots \right] dy$$

$$- \int_0^{\delta} \rho_v U_v \big|_x \, dy$$

$$= \int_0^{\delta+d\delta} \frac{\partial}{\partial x}(\rho_v U_v)\cdot dx \cdot dy + \int_{\delta}^{\delta+d\delta} \rho_v U_v \, dy$$

$$= -\int_0^{\delta+d\delta} \frac{\partial}{\partial y}(\rho_v V_v) \, dx \cdot dy + \int_{\delta}^{\delta+d\delta} \rho_v U_v \cdot dy$$

($\because$ From continuity equation

$$\frac{\partial}{\partial x}(\rho_v U_v) = -\frac{\partial}{\partial y}(\rho_v V_v))$$

$$= -\rho_v V_v]_0^{\delta + d\delta} dx + \rho_v \cdot U_v \cdot d\delta$$

$$= -\rho_v V_v|_{int} dx + 0 + \rho_v U_v|_{int}^{d\delta}$$

$$= (\rho_v U_v \cdot d\delta - \rho_v \cdot V_v \cdot dx)_{interface}$$

Therefore net flow rate of vapour per unit length

$$= \rho_v U_v \frac{d\delta}{dx} - \rho_v V_v$$

Now, substituting these expressions in the equation (B-5), we get the equation (2.23).

$$\rho_v \cdot \frac{d\delta}{dt} = \frac{1}{h_{fg}} [q_R - \frac{K_v}{\delta} \cdot \frac{\partial T_v}{\partial \eta} + \frac{K_L}{\delta} \cdot \frac{\partial T_L}{\partial \eta}]$$

$$- (\rho_v U_v \frac{d\delta}{dx} - \rho_v V_v) \qquad (2.23)$$

APPENDIX C

All the thermophysical properties are functions of temperature. The equations for the variation of properties are obtained from Sabhapathy (1980), Kothandaraman (1975), and steam tables - ERA (1967). All the property values are taken in SI units.

The equations that are used for the calculation of thermophysical properties are:

$$\rho_V = 219.5/T \qquad T \text{ in } {}^{\circ}K$$

$$\mu_V = (80.4 + 0.407 \, (T-273.0)) \times 10^{-7} \text{ for } T < 973^{\circ}K$$

$$= (366.7 + 0.523 \, (T-973)) \times 10^{-7} \text{ for } T \geq 973^{\circ}K$$

$$K_V = 0.0022 + 0.000098 \, (T-350) \qquad \text{for } T \leq 650^{\circ}K$$

$$= 0.058 + 0.000145 \, (T-650) \qquad \text{for } T \geq 650^{\circ}K$$

$$C_{p_V} = (0.4432 - 2.8532 \times 10^{-5}T + 1.9848 \times 10^{-7} \, T^2$$
$$- 6.6372 \times 10^{-11} \, T^3) \times 4186.8$$

$$\rho_L = 972.0 + (353.0 - T) \times 0.69984$$

$$\mu_L = (4.701 + 0.0916 \, (333 - T)) \times 10^{-4} \text{ for } T \leq 333^{\circ}K$$

$$= (3.556 + 0.05725(353 - T)) \times 10^{-4}$$

$$\text{for } 333^{\circ}K \leq T \leq 353^{\circ}K$$

$$= (2.821 + 0.03518 \, (373.0 - T)) \, 10^{-4} \text{ for}$$

$$\text{for } 353^{\circ}K \leq T \leq 373^{\circ}K$$

$$K_L = (668.7 - 0.87 \ (353-T))10^{-4} \quad \text{for } 333°K \leq T \leq 353°K$$
$$= (628.0 - 1.16 \ (333 - T)) \ 10^{-4} \quad \text{for } T \leq 333°K$$
$$= (680.4 - 0.555(373.0-T)) \ 10^{-4} \quad \text{for } 353°K \leq T \leq 373°K$$

$$C_{p_v} = (2.1397 - 9.6814 \times 10^{-3} \times T$$
$$+ 2.6854 \times 10^{-5} \times T^2 - 2.4134 \times 10^{-8} \times T^3) \times 4186.8$$

The density is in kg/m^3, coefficient of viscosity in kg/m-s, the thermal conductivity in w/m$°$K and the specific heat in J/kg$°$K. For non-dimensional form of these property variations refer to the program listing.

APPENDIX   D

Here, an approximate stability criterion which limits
the allowable timestep is given. Eventhough, the criterion
given below applies only to single-phase flows, it is inte-
resting to note that it predicts the timestep satisfactorily
to the present two-phase flow problem.

The stability requirement of a two-dimensional advection-
diffusion equation with upwind differencing was given (Patrick
J. Roache, 1972) as

$$\Delta t \lesssim \frac{1}{2\alpha \left(\frac{1}{\Delta x^2} + \frac{1}{\Delta y^2} \right) + \frac{|U|}{\Delta x} + \frac{|V|}{\Delta y}}$$

Substituting various values in the above inequality ($\Delta x = 0.001$ m,
$\Delta y = 5.45 \times 10^{-5}$ m, $\alpha_{vs} = 0.0692/3600$, $|U| = 0.5661 \times 20$ m/sec,
$|V| = 0.005832 \times 20$ m/sec.) we can write it as

$$\Delta t \lesssim \frac{1}{38.44 + 12944.0 + 11320.0 + 2139.0}$$

$$\lesssim \frac{1}{26441.4}$$

$$\leq 37.8 \text{ micro seconds}$$

And the allowable timestep found numerically for the set
of values given above is 20 micro seconds. So, the predicted
value from the above inequality is comparable with the

actual timestep stipulated by stability of the scheme. By
looking at the order of magnitude of each term in the above
inequality it can be concluded that Δy has a pronounced
effect (two-fold) on Δt. So, as we proceed further seeking
solution at downstream regions the dimensional value of Δy
is increasing and this could lead to increase the allowable
timestep at downstream regions. This is consistent with the
remark made in section (3.3). Eventhough at downstream regions,
U is larger (thus decreases the allowable timestep at down-
stream regions) its effect is offset by the decrease in V
and a dominant two-fold effect of increase in Δy at downstream
regions. The net effect is to increase Δt at downstream
regions.

It was mentioned that the timestep was limited by
stability on vapour-side. This is easy to understand because
the velocities in vapour-region are much larger than the
velocities in liquid region. Thus the last two terms in the
inequality are small in liquid region which implies that a
relatively large time step can be used in liquid region.

APPENDIX E

Transformation of non-linear abscissa (used by Nishikawa et.al. (1976)) to a more convenient y/δ coordinate is shown in this appendix. Nishikawa et.al. used the non-linear abscissa $\tilde{n}_V$ which is defined as follows.

$$\tilde{n}_V = \frac{n_V(y)}{n_V(\delta)} \qquad \text{where} \qquad n_V(y) = \frac{C_V}{x^{1/4}} \int_0^y \frac{\rho_V}{\rho_{VS}} \cdot dy$$

Let $\rho_V \sim \frac{1}{T}$, where T is the absolute temperature in $^\circ K$.

$$\therefore \quad n_V = \frac{C_V}{x^{1/4}} \int_0^y \frac{T_{VS}}{T} \, dy$$

and T, the temperature at any location y, is assumed to be linear function of y, for brevity (See Fig. (4.2b) for the actual temperature variation).

i.e., $\quad T = T_W + y/\delta \, (T_{VS} - T_W)$

$$\therefore \quad n_V(y) = \frac{C_V}{x^{1/4}} \int_0^y \frac{dy}{T_W/T_{VS} + \frac{y}{\delta}(1-T_W/T_{VS})}$$

$$= \frac{C_V}{x^{1/4}} \frac{T_{VS}}{T_W} \left[\int_0^y \frac{\frac{dy}{T}}{1 + \frac{y}{\delta}(\frac{T_{VS}}{T_W} - 1)} \right]$$

$$\therefore \quad n_V(y) = \frac{C_V}{x^{1/4}} \frac{T_{VS}}{T_W} \cdot \ln\left[1 + \frac{y}{\delta}(\frac{T_{VS}}{T_W} - 1)\right] \cdot \frac{\delta}{(\frac{T_{VS}}{T_W} - 1)}$$

$$\therefore \quad \frac{n_V(y)}{n_V(\delta)} = \tilde{n}_V = \frac{\ln\left[1+(y/\delta)\left(\frac{T_{VS}}{T_W}-1\right)\right]}{\ln\left(T_{VS}/T_W\right)} \quad \text{and}$$

$$\frac{y}{\delta} = \left[\left(\frac{T_{VS}}{T_W}\right)^{\tilde{n}_V} - 1\right] / \left[\frac{T_{VS}}{T_W} - 1\right]$$

APPENDIX F

1. Average Nusselt Number:

$$Nu_{average} = \frac{\bar{h} L}{K_{vs}} \quad \text{where} \quad \bar{h} = \frac{1}{L} \int_0^L h \, dx$$

and $\quad h = h_{convection} + h_{radiation} = h_c + h_r$

Also $h_c \, x^{1/4}$ is constant irrespective of x, because of the similarity shown by Nishikawa et.al. (1976) for no radiation film boiling problem. $h_c x^{1/4}$ is calculated for various x values in the present work and it is found to be fairly constant away from the leading edge. The deviation of $hx^{1/4}$ at the leading edge from the constant value at the downstream is not more than 6 percent. This is because of the leading edge singularity problems in most of the numerical schemes. However, this can be totally eliminated by reducing the grid size near the leading edge and thus dividing the length of the plate into more number of divisions. In the present work $h_c x^{1/4}$ is approximated to be constant all along the length of the plate and thus the local conductive-convective heat transfer coefficient h_c is calculated as follows.

$$h_c = \frac{hc \, x^{1/4}}{x^{1/4}}$$

$$= \frac{\text{Constant (a value taken at the end of the plate)}}{x^{1/4}}$$

(F1)

Also, it was observed that the value of $h_c \, x^{1/4}$ is constant within the accuracy of 8 percent even when radiation is included. Thus, even when radiation is included in the numerical scheme, h_c is calculated from the equation (F1). Hereafter, we refer to h_c as the local conductive-convective heat transfer coefficient when radiation is included and h_{co} as the local conductive-convective heat transfer coefficient when radiation is absent.

2. Comparison of Results with those of Sparrow (1964):

Sparrow had given the ratio of q/q_0 as a function of $X =$

$$[\, g \, \rho_L \, \lambda^* / (16 \, \nu \, K \, T_w - T_{vs})]^{1/3} \cdot x \quad \text{for various values of}$$

$$N_1 \;=\; \frac{h_r}{K} \left[\frac{16 \, \nu \, K \, (T_w - T_{vs})}{g \, \rho_L \, \lambda^*} \right]^{1/3}$$

$$h_r \;=\; \sigma \, (T_w^2 + T_{vs}^2) \, (T_w + T_{vs})$$

and $\qquad \lambda^* = \lambda \left[1 + \dfrac{0.84 \, C_p \, (T_w - T_{vs})}{\lambda \, P_r} \right]$

For $T_w - T_{vs} = 800$ K, $\qquad N_1 = 0.31696$

(after substituting values of all other parameters at saturation temperature in the expression for N_1)

and $\qquad X \;=\; 200 \quad$ corresponds to $x = 1.1$ cms.

For $X = 200$ and $N_1 \simeq 0.31$ q/q_0 was given by Sparrow as $\simeq 1.92$. From the present analysis $q/q_0 = (h_c + h_r)/h_{co} \simeq 1.66$.

3. Bromley's Thumb Rule for Accounting Radiation:

Bromley's thumb rule for accounting radiation in saturated boiling can be derived as follows.

$$\dot{m}^* \ \alpha \ h.\Delta T \qquad \text{and} \qquad \dot{m} \ \alpha \ h_{co} \ \Delta T$$

therefore, $\qquad \dot{m}^*/\dot{m} \ \underset{\sim}{} \ h/h_{co}$

Also, $\qquad \dot{m} \ \alpha \ \delta^3,$

therefore, $\qquad \dot{m}^*/\dot{m} \ \underset{\sim}{} \ \delta^*/\delta^3 \ \underset{\sim}{} \ h/h_{co}$

$$\delta/\delta^* = (h_{co}/h)^{1/3} \quad \text{and}$$

$$h = h_c + h_r = \frac{K}{\delta^*} + h_r = \frac{K}{\delta} \cdot \frac{\delta}{\delta^*} + h_r$$

But $\qquad K/\delta = h_{co}$

therefore, $\quad h = h_{co} \cdot \frac{\delta}{\delta^*} + h_r = h_{co} \ (\frac{h_{co}}{h})^{1/3} + h_r$

This implies that,

$$h = h_c + h_r = h_{co} \ (\frac{h_{co}}{h_c + h_r})^{1/3} + h_r$$

$$h_c = h_{co} \ (\frac{h_{co}}{h_c + h_r})^{1/3}$$

$$h_c = h_{co} \ (\frac{h_{co}}{h_c + h_r})^{1/3}$$

$$\frac{h_c}{h_{co}} = (\frac{h_{co}}{h_c + h_r})^{1/3} \qquad\qquad \text{(F2)}$$

This is the condition to be verified to affirm Bromley s intuitive rule for accounting radiation. Both the LHS and RHS quantities in the equation (F2) are evaluated, using the results of the present work, and compared. Comparison of these two quantities is shown in table.

Table F-1: Verification of Bromley s Rule.

Location (Distance from the leading edge) (mm)	$\Delta T_v = 400$		$\Delta T_v = 800$	
	h_c/h_{co}	$\{h_{co}/(h_c+h_r)\}^{1/3}$	h_c/h_{co}	$\{h_{co}/(h_c+h_r)\}^{1/3}$
6	0.9581	0.9437	0.9181	0.9128
7	0.9566	0.9413	0.9160	0.9090
8	0.9551	0.9392	0.9144	0.9058
9	0.9538	0.9372	0.9126	0.9028
10	0.9526	0.9355	0.9113	0.9001
11	0.9518	0.9339	0.9100	0.8978
12	0.9508	0.9324	0.9087	0.8955
13	0.9498	0.9311	0.9077	0.8934
14	0.9489	0.9298	0.9065	0.8919
15	0.9481	0.9286	0.9056	0.8896

4. Transformation of the Present Flat Plate Results to Horizontal Cylinders:
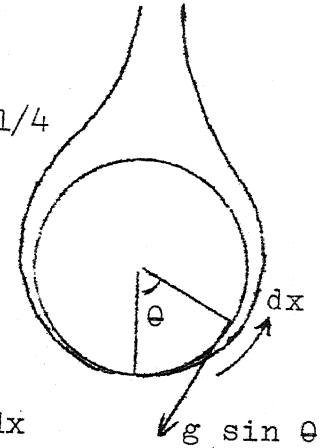
$$h_{cylinder} = h_{c\ cylinder} + h_{rad}$$

But
$$h_{c\ cylinder} = h_{c\ flat\ plate}\ (\sin \theta)^{1/4}$$

$$= h_c\ (\sin \theta)^{1/4}$$

$$\bar{h}_{c\ cylinder} = \frac{2}{\pi D} \int_0^{\pi D/2} h_{c\ cylinder}\ dx$$

$$= \frac{2}{\pi D} \int_0^{\pi D/2} h_c\ (\sin \theta)^{1/4}.dx$$

$$\bar{h}_{c\ cylinder} = \frac{2}{\pi D} \int_0^{\pi D/2} h_c\ (\sin (x/R))^{1/4}\ dx$$

$$= \frac{2}{\pi D} \cdot h_c x^{1/4} \int_0^{\pi D/2} [\frac{\sin\ (x/R)}{x}]^{1/4}\ dx$$

and
$$\bar{h}_{c\ cylinder} \cdot D^{1/4} = \frac{2}{\pi D} \cdot D^{1/4}\ (h_c\ x^{1/4})\ \{$$

$$\int_0^{\pi D/2} [\frac{\sin\ (x/R)}{x}]^{1/4}.dx\}$$

Now define,
$$2x/\pi D = \tilde{x}\ ,\quad x^{1/4} = \tilde{x}^{1/4}\ (\frac{\pi D}{2})^{1/4}$$

$$\bar{h}_{c\ cylinder} \cdot D^{1/4} = (h_c\ x^{1/4})\ D^{1/4}.(\frac{2}{\pi D})^{1/4}\ \{$$

$$\int_0^1 [\frac{\sin \pi \tilde{x}}{\tilde{x}}]^{1/4}\ d\tilde{x}$$

$$= h_c\ x^{1/4}\ (\frac{2}{\pi})^{1/4} \int_0^1 \frac{\sin(\pi \tilde{x})^{1/4}}{\tilde{x}^{1/4}}.d\tilde{x}$$

$$= \frac{1}{1.03} \cdot h_c\ x^{1/4}$$

$$\bar{h}_{cylinder} \cdot D^{1/4} = \bar{h}_{c\ cylinder} \cdot D^{1/4} + h_{rad} \cdot D^{1/4}$$

$$= \frac{1}{1.03} h_c\ x^{1/4} + h_{rad}\ D^{1/4} \qquad (F3)$$

The following table shows the error in the prediction of average heat transfer coefficient for cylinders of various diameters.

Table F-2: Comparison of present results with experimental data.

Diameter of cylinder (mm)	ΔT_L (°K)	ΔT_v (°K)	Experimental value	Present work (ε=1)	Percent error in present result	Numerical result by Nishikawa et.al.	Percent error in their result
13.0	0	250	204.5	188	-8.06	154	-24.69
		300	197.47	191	-3.27	153	-22.51
		425	190.4	204	+7.14	152	-20.16
		500	199.8	215	+7.60	152	-23.92
6.0	0	300	188.21	218	+15.82	188.2	0
		400	188.21	226	+20.07	185.0	-1.70
		600	201.05	260	+29.32	186.0	-7.46
16.0	20	700	254.43	276.0	+8.47	200.86	-21.0
		800	263.35	300.53	+14.11	194.17	-26.37

```
C     THE FOLLOWING ARE THE DIRECTIONS TO MAKE USE OF THE PROGRAM.
C     THIS PROGRAM IS FOR SUBCOOLED BOILING WITH RADITION
C     I AND J ARE SPECIFICATION OF A GRID POINT ALONG STREAMWISE AND
C     CROSS STREAM DIRECTIONS RESPECTIVELY.
C     NOTE: ALL VARIABLES ARE NON-DIMENSIONALISED
C     DEL(I) = VAPOUR LAYER THICKNES AT LOCATION I
C     DELD(I) = A DUMMY LOCATION FOR NEWLY CALCULATED DEL(I)
C     UG(I,J),UL(I,J)  ARE VELOCITIES ALONG THE PLATE IN GAS AND
C     LIQUID REGIONS RESPECTIVELY.
C     VG(I,J),VL(I,J)  ARE VELOCITIES NORMAL TO PLATE IN GAS AND
C     LIQUID REGIONS RESPECTIVELY.
C     TG(I,J),TL(I,J) ARE TEMPERATURES IN GAS AND LIQUID REGIONS
C     RESPECTIVELY.
C     PGS,KGS,MUGS,CPGS ARE VAPOUR PROPERTIES AT SATURATION
C     TEMPERATURE
C     PLS,KLS,MULS,CPLS ARE LIQUID PROPERTIES AT SATURATION
C     TEMPERATURE
C     DX  AND  DY  ARE THE SPACE STEPS IN X AND Y
C     DIRECTIONS RESPECTIVELY AND  DT  IS THE TIME STEP
C     BETA AND OMEGA ARE RELAXATION PARAMETERES
C     K  AND  N  REPRESENT THE NUMBER OF DIVISIONS MADE IN THE
C     X-DIRECTION AND VAPOUR BOUNDARY LAYER RESPECTIVELY.
C     M=M = NUMBER OF DIVISIONS MADE IN THE LIQUID BOUNDARY LAYER
C     ALL PROPERTIES ARE IN SI UNITS
C     TW = WALL TEMPERATURE     TGS = TLS = SATURATION TEMPERATURE
C     TM = TEMPERATURE OF THE STAGNANT LIQUID (AT INFINITY)
C     PLM = DENSITY OF STAGNANT LIQUID (AT INFINITY)
C     --CONVEG--IS THE CONVECTION VELOCITY IN THE VAPOUR
C     --GRAG----IS THE GRASHOFF NUMBER OF GAS
C     JAG=JACOB NUMBER OF GAS          PEG=PECLET NUMBER OF GAS
C     JAL=JACOB NUMBER OF LIQUID       PEL=PECLET NUMBER OF LIQUID
      DIMENSION DEL(0:15),UG(0:1,0:10),UL(0:1,0:40),DELD(0:15),
     1TG(0:1,0:10),TL(0:1,0:40),VG(0:1,0:10),VL(0:1,0:40)
      REAL MUGS,MULS,KGS,KLS,NUGS,NULS,JAL,JAG,BETRLD
     1,GRYGL,MUGP1,MULP3,MULP4,KGP2,KLP5,KLPS,VGLIP1,MGLJ
     1,KLTJP1,KLTI,MLTJP1,MLTI,KGTJP1,KGTI
      DX=0.04
      DY=0.10
C     READ THE TIME STEP & NO.ITERATIONS FROM THE FILE(FOR21.DAT)
      READ(21,*)DT,ITND
      BETA=350.0
      OMEGA=350.0
      K=15
      M=40
      N=10
      G=9.81
      TW=1173.0
      TGS=373.0
      TLS=373.0
      PLM=973.0
      TM=353.0
      PGS=0.598
      PLS=950.0
      MUGS=1.496E-05
      NUGS=2.0E-05
      MULS=2.81E-04
      NULS=0.293E-06
      KGS=0.02373
      KLS=0.6804
      CPGS=2073.0
      CPLS=4216.0
      ALGS=0.0692/3600.0
      ALLS=KLS/(PLS*CPLS)
      HFG=540.0*4186.8
      PRG=NUGS/ALGS
```

```
            PRL=MULS/ALLS
            CONST=1.0
            CONVEG=(G*(PLM-PGS)*0.025/PGS)**0.5
            STGMA=5.67E-08
            EMTSST=0.8
C     IF YOU WANT TO INCLUDE RADIATION DELETE C?? IN THE NEXT LINE
            ROND=EMTSST*(TW**4.0-TGS**4.0)*STGMA/(HFG*PGS*CONVEG)
            GRAG=(G*(PLM-PGS)*0.025**3.0)/(PGS*MUGS**2.0)
            JAL=CPLS*(TLS-TW)/HFG
            PRL=CONVEG*0.025/ALLS
            JAG=CPGS*(TW-TGS)/HFG
            PRG=CONVEG*0.025/ALGS
C     THE FOLLOWING STATEMENTS WILL READ THE 'INITIAL DATA'
C     THE INITIAL DATA 'SHOULD' BE IN A FILE IN PRESCRIBED FORM
C     THAT FILE NAME SHOULD BE       FOR20.DAT
930         DO 900 I=0,1
            DO 905 N=0,1
            NA=5*N
905         READ(20,*)(HG(I,J),J=NA,NA+4)
            READ(20,*)HG(I,10)
            DO 906 N=0,1
            NA=5*N
906         READ(20,*)(VG(I,J),J=NA,NA+4)
            READ(20,*)VG(I,10)
            DO 907 N=0,1
            NA=5*N
907         READ(20,*)(TG(I,J),J=NA,NA+4)
            READ(20,*)TG(I,10)
            DO 908 N=0,5
            NA=5*N+10
908         READ(20,*)(UL(I,J),J=NA,NA+4)
            READ(20,*)UL(I,40)
            DO 909 N=0,5
            NA=5*N+10
909         READ(20,*)(VL(I,J),J=NA,NA+4)
            READ(20,*)VL(I,40)
            DO 911 N=0,5
            NA=5*N+10
911         READ(20,*)(TL(I,J),J=NA,NA+4)
            READ(20,*)TL(I,40)
            DO 910 N=0,2
            NA=5*N
910         READ(20,*)(DEL(ID),ID=NA,NA+4)
900         READ(20,*)DEL(15)
575         ONEBDX=1.0/DX
            ONEBDT=1.0/DT
            ONBMGS=1.0/MUGS
            OBKGS=1.0/KGS
            OBCPGS=1.0/CPGS
            ONBPLS=1.0/PLS
            ONBMLS=1.0/MULS
            OBKLS=1.0/KLS
            OBCPLS=1.0/CPLS
            DENSTY=219.5/PGS
            DEGSUP=TW-TLS
            DEGSUB=TLS-TW
            GRYGL=MUGS/(MUGS+MULS)
            LRYGL=MULS/(MULS+MUGS)
            KGP1=(973.0-TLS)/DEGSUP
            KGP2=(650.0-TLS)/DEGSUP
            MULP3=(333.0-TW)/DEGSUB
            MULP4=(353.0-TW)/DEGSUB
            KLP5=(333.0-TW)/DEGSUB
            KLP6=(353.0-TW)/DEGSUB
            PRTERM=G*0.025/(CONVEG*CONVEG*PLS)
```

G-2

```
      PRATIO=PGS/PLS
      THCOD1=NULS/(PRL*0.025*CONVEG*(DY*DY))
      DYSSOG=(DY*DY*SQRT(GRAG))
      DYSCLN=NULS/(CONVEG*DY*DY*0.025)
      CODGS1=TAG/(DY*PEG)
      CODL1=TAL*PLS/(PEL*PGS*DY)
      THCOG1=PRG*DYSSOG
C     NUMBER OF ITERATIONS IS DENOTED BY "IC"
1111  DO 40 IC=1,ITNO
      N=10
C     THE FOLLOWING 'IF' STATEMENTS WILL CHECK THE VALUES OF VARIABLES
C     BEFORE START OF EACH ITERATION.IF TEMPERATURE EXCEEDS SAY.10.0
C     THE SCHEME SHOULD COME TO A STOP(BECAUSE A MAX. VALUE IS 1.0).
      IF(ABS(TG(I,9)).GT.10.0) GO TO 700
      IF(ABS(TL(1,11)).GT.10.0) GO TO 700
531   DO 50 I=1,1
      DELISQ=DEL(I)*DEL(I)
      DLTIM1=DEL(I)-DEL(I-1)
      DBDLDX=1.0/(DEL(I)*DX)
      DBDLDY=1.0/(DEL(I)*DY)
      DYESSG=DYSSOG*DELISQ
      EYSCLN=DYSCLN/DELISQ
      THCOD2=THCOD1/DELISQ
      DELDY=DEL(I)*DY
      CODGS2=CODGS1/DEL(I)
      CODL2=CODL1/DEL(I)
      CONXGL=DLTIM1*DBDLDX
      THCOG2=THCOG1*DELISQ
C     MOMENTUM EQUATION ON THE VAPOUR SIDE
      IF(TG(I,1).GE.MUGP1) GO TO 1000
      MGTJ=DNBMGS*(80.4+0.407*(TG(I,1)*DEGSUP+(TLS-273.0)))*
     11.0E-07
      GO TO 1001
1000  MGTJ=DNBMGS*(366.7+0.623*(TG(I,1)*DEGSUP+(TLS-973.0)))*
     11.0E-07
1001  DO 55 J=1,N-1
      IF(TG(I,J+1).GE.MUGP1) GO TO 1002
      MGTJP1=DNBMGS*(80.4+0.407*(TG(I,J+1)*DEGSUP+(TLS-273.0)))*
     11.0E-07
      GO TO 1003
1002  MGTJP1=DNBMGS*(366.7+0.623*(TG(I,J+1)*DEGSUP+(TLS-973.0)))*
     11.0E-07
1003  PGTJ=DENSTY/(DEGSUP*TG(I,J)+TLS)
      UGCONX=UG(I,J)*(UG(I,J)-UG(I-1,J))*DNBRDX-UG(I,J)*(UG(I,J+1)-
     2UG(I,J))*FLOAT(J)*CONXGL
      UGCONY=VG(I,J)*(UG(I,J+1)-UG(I,J))*DBDLDY
      UGPRE=(PLM-PGTJ*PGS)/((PLM-PGS)*PGTJ)
      UGVISY=(MGTJP1*(UG(I,J+1)-UG(I,J))-
     5MGTJ*(UG(I,J)-UG(I,J-1)))/
     6(DYESSG*PGTJ)
      UG(I,J)=UG(I,J)+DT*(-UGCONX-UGCONY+UGPRE+UGVISY)
      MGTJ=MGTJP1
      IF(IC.NE.ITNO) GO TO 55
      DUGDT=-UGCONX-UGCONY+UGPRE+UGVISY
      PRINT*,I,J,DUGDT,UGCONX,UGCONY,UGPRE,UGVISY
55    CONTINUE
C     MOMENTUM EQUATION ON LIQUID SIDE
8888  IF(TL(I,N+1).GE.MULP3) GO TO 1004
      MLTJ=DNBMLS*(4.701+0.0916*((333.0-TM)-TL(I,N+1)*DEGSUB))*
     10.0001
      GO TO 888
1004  IF(TL(I,N+1).GE.MULP4) GO TO 1006
      MLTJ=DNBMLS*(3.556+0.05725*((353.0-TM)-TL(I,N+1)*DEGSUB))*
     20.0001
      GO TO 888
```

```
1006      MLTJ=DNBMLS*(2.821+0.03518*((373.0-TM)-TL(I,N+1)*DEGSUB))*
          40.0001
888       DO 65 J=N+1,M-1
          PLTJ=DNBPLS*(972.0+(353.0-TM-TL(I,J)*DEGSUB)*7.2*0.0972)
          IF(TL(I,J+1).GE.MULP3) GO TO 1007
          MLTJP1=DNBMLS*(4.701+0.0916*((333.0-TM)-TL(I,J+1)*DEGSUB))*
          10.0001
          GO TO 1009
1007      IF(TL(I,J+1).GE.MULP4) GO TO 1008
          MLTJP1=DNBMLS*(3.556+0.05725*((353.0-TM)-TL(I,J+1)*DEGSUB))*
          20.0001
          GO TO 1009
1008      MLTJP1=DNBMLS*(2.821+0.03518*((373.0-TM)-TL(I,J+1)*DEGSUB))*
          40.0001
1009      IF(VL(I,J).GT.0.0) GO TO 5610
          ULCONX=UL(I,J)*(UL(I,J)-UL(I-1,J))*DNEBOX-UL(I,J)*(UL(I,J)-
          2UL(I,J-1))*FLOAT(J)*CONXGL
          ULCONY=VL(I,J)*(UL(I,J)-UL(I,J-1))*DBDGDY
          GO TO 5611
5610      ULCONY=VL(I,J)*(UL(I,J+1)-UL(I,J))*DBDGDY
          ULCONX=UL(I,J)*(UL(I,J)-UL(I-1,J))*DNEBOX-UL(I,J)*(UL(I,J+1)-
          2UL(I,J))*FLOAT(J)*CONXGL
5611      ULPRE=PRTER4*(PLM-PLTJ*PLS)/PLTJ
          ULVISY=(MLTJP1*(UL(I,J+1)-UL(I,J))-
          4MLTJ*(UL(I,J)-UL(I,J-1))*EVSCLN/PLTJ
          UL(I,J)=UL(I,J)+BETA*DT*(-ULCONX-ULCONY+ULPRE+ULVISY)
          MLTJ=MLTJP1
          IF(IC.NE.ITND) GO TO 65
          ULSUM=-ULCONX-ULCONY+ULPRE+ULVISY
          IF(J.GT.15) GO TO 65
          PRINT*,I,J,ULSUM,ULCONX,ULCONY,ULPRE,ULVISY
65        CONTINUE
C         MATCHING OF SHEAR STRESS AT THE INTERFACE
          UG(I,N)=GBVGL*UG(I,N-1)+LBVGL*UL(I,N+1)
          UL(I,N)=UG(I,N)
C         ENERGY EQUATION ON THE VAPOUR SIDE
          IF(TG(I,1).GE.KGP2) GO TO 1010
          KGTJ=DBKGS*(0.0222+0.0000987*(TG(I,1)*DEGSUP+TLS-350.0))
          GO TO 200
1010      KGTJ=DBKGS*(0.0518+0.000145*(TG(I,1)*DEGSUP+TLS-650.0))
200       DO 100 J=1,N-1
          IF(TG(I,J+1).GE.KGP2) GO TO 1011
          KGTJP1=DBKGS*(0.0222+0.0000987*(TG(I,J+1)*DEGSUP+TLS-350.0))
          GO TO 1012
1011      KGTJP1=DBKGS*(0.0518+0.000145*(TG(I,J+1)*DEGSUP+TLS-650.0))
1012      CPGTJ=4186.8*DBCPGS*(0.44322-(2.85391E-05)*(TG(I,J)*DEGSUP+TLS)
          1+(1.98477E-07)*(TG(I,J)*DEGSUP+TLS)**2.0-(6.66372E-11)*
          2(TG(I,J)*DEGSUP+TLS)**3.0)
          PGTJ=DENSTY/(DEGSUP*TG(I,J)+TGS)
          TGCONX=UG(I,J)*(TG(I,J)-TG(I-1,J))*DNEBOX-UG(I,J)*(TG(I,J+1)-
          2TG(I,J))*FLOAT(J)*CONXGL
          TGCONY=VG(I,J)*(TG(I,J+1)-TG(I,J))*DBDGDY
          TGCODY=(KGTJP1*(TG(I,J+1)-TG(I,J))-
          4KGTJ*(TG(I,J)-TG(I,J-1)))/
          5(THCOG2*PGTJ*CPGTJ)
          TG(I,J)=TG(I,J)+DT*(-TGCONX-TGCONY+TGCODY)
          KGTJ=KGTJP1
          IF(IC.NE.ITND) GO TO 100
          DTGDT=-TGCONX-TGCONY+TGCODY
          PRINT*,IC,I,J,DTGDT,TGCONX,TGCONY,TGCODY
100       CONTINUE
C         ENERGY EQUATION ON LIQUID SIDE
7979      IF(TL(I,N+1).GE.KLP5) GO TO 1099
          KLTJ=DBKLS*(628.0-1.16*(333.0-TM-TL(I,N+1)*DEGSUB))*0.001
          GO TO 747
```

G-4

```
1099      IF(TL(I,N+1).GE.KLP6) GO TO 1015
          KLTI=DBKLS*(668.7-0.87*(353.0-TM-TL(I,N+1)*DEGSUB))*0.001
          GO TO 747
1015      KLTI=DBKLS*(680.4-0.555*((373.0-TM)-TL(I,N+1)*DEGSUB))*0.001
747       DO 222 J=N+1,M-1
          IF(TL(I,J+1).GE.KLP5) GO TO 2013
          KLTJP1=DBKLS*(628.0-1.16*(333.0-TM-TL(I,J+1)*DEGSUB))*0.001
          GO TO 7479
2013      IF(TL(I,J+1).GE.KLP6) GO TO 2015
          KLTJP1=DBKLS*(668.7-0.87*(353.0-TM-TL(I,J+1)*DEGSUB))*0.001
          GO TO 7479
2015      KLTJP1=DBKLS*(680.4-0.555*((373.0-TM)-TL(I,J+1)*DEGSUB))*0.001
7479      CPLIJ=4186.8*DBCPLS*(2.13974-(9.68137E-03)*(TL(I,J)*DEGSUB+TM)
         1+(2.58536E-05)*(TL(I,J)*DEGSUB+TM)**2.0-(2.42139E-08)*(TL(I,J)
         2*DEGSUB+TM)**3.0).
          PLIJ=DNBPLS*(972.0+(353.0-TM-TL(I,J)*DEGSUB)*7.2*0.0972)
          IF(VL(I,J).LT.0.0) GO TO 5612
          TLCONX=UL(I,J)*(TL(I,J)-TL(I-1,J))*DNEBDX-UL(I,J)*(TL(I,J)-
         2TL(I,J-1))*FLOAT(J)*CONXGL
          TLCONY=VL(I,J)*(TL(I,J)-TL(I,J-1))*DBYDY
          GO TO 5613
5612      TLCONY=VL(I,J)*(TL(I,J+1)-TL(I,J))*DBDYDY
          TLCONX=UL(I,J)*(TL(I,J)-TL(I-1,J))*DNEBDX-UL(I,J)*(TL(I,J+1)-
         2TL(I,J))*FLOAT(J)*CONXGL
5613      TLCODY=(KLTJP1*(TL(I,J+1)-TL(I,J))-
         4KLTI*(TL(I,J)-TL(I,J-1)))*THCDD2/(CPLIJ*CPLIJ)
          TL(I,J)=TL(I,J)+OMEGA*DT*(-TLCONX-TLCONY+TLCODY)
          KLTI=KLTJP1
          IF(IC.NE.ITND) GO TO 222
          DTDT=-TLCONX-TLCONY+TLCODY
          IF(J.GT.15) GO TO 222
          PRINT*,IC,I,J,DTDT,TLCONX,TLCONY,TLCODY
222       CONTINUE
C         CONTINUITY EQUATION ON VAPOUR SIDE
201       PGIJM1=DENSTY/(DEGSUP*TG(1,J)+TGS)
          DO 160 J=1,N
          PGIJ=DENSTY/(DEGSUP*TG(I,J)+TGS)
          PGIM1J=DENSTY/(DEGSUP*TG(I-1,J)+TGS)
          PART1=(PGIJ*UG(I,J)-PGIM1J*UG(I-1,J))*DNEBDX
          PART2=(PGIJ*UG(I,J)-PGIJM1*UG(I,J-1))*FLOAT(J)*CONXGL
          DUBYDX=PART1-PART2
          VG(I,J)=(PGIJM1*VG(I,J-1)-DELDY*DUBYDX)/PGIJ
          PGIJM1=PGIJ
160       CONTINUE
C         FINDING THE BOUNDARY LAYER THICKNESS
          CODGAS=TG(I,N-1)*CODGS2
          CODLIQ=(1.0-TL(I,N+1))*CODL2
          NETFLO=UG(I,N)*DLTIM1*DNEBDX-VG(I,N)
          VAPGEN=CODGAS-CODLIQ+RDN2
          IF(IC.NE.ITND) GO TO 757
          PRINT*,CODGAS,CODLIQ,VAPGEN,NETFLO
757       DSUM=DEL(I)+DT*(VAPGEN-NETFLO)
          DELD(I)=DSUM
C         FINDING THE VELOCITY AT THE INTERFACE IN LIQUID REGION
746       PART1=UL(I,N)*(DEL(I)-DEL(I-1))*DNEBDX
          PART2=PRATIO*(VG(I,N)-UG(I,N)*(DEL(I)-DEL(I-1))*DNEBDX)
          VL(I,N)=PART1+PART2
C         CONTINUITY EQUATION ON THE LIQUID SIDE
467       PLIJM1=DNBPLS*(972.0+(353.0-TM-TL(I,N)*DEGSUB)*7.2*0.0972)
          DO 190 J=N+1,M-1
          PLIJ=DNBPLS*(972.0+(353.0-TM-TL(I,J)*DEGSUB)*7.2*0.0972)
          PLIM1J=DNBPLS*(972.0+(353.0-TM-TL(I-1,J)*DEGSUB)*7.2*0.0972)
          PART1=(PLIJ*UL(I,J)-PLIM1J*UL(I-1,J))*DNEBDX
          PART2=(PLIJ*UL(I,J)-PLIJM1*UL(I,J-1))*FLOAT(J)*CONXGL
          DUBYDX=PART1-PART2
```

G-5

```
          VL(I,J)=(PLTIM1*VL(I,J-1)-DELDY*DUBYDX)/PLTJ
          PLTIM1=PLTJ
120       CONTINUE
50        CONTINUE
C         ASSIGNING THE DUMMY B.L.THICKNESS TO THE RUNNING VARIABLE
          DO 444 I=1,1
          DEL(I)=DELD(I)
444       CONTINUE
40        CONTINUE
C         THE FOLLOWING STATEMENTS WILL PRINT ALL THE VARIABLES
C         AFTER THE PRESCRIBED NO. OF ITERATIONS.
          DO 500 I=0,1
          DO 505 N=0,1
          NA=5*N
505       PRINT*,(UG(I,J),J=NA,NA+4)
          PRINT*,UG(I,10)
          DO 506 N=0,1
          NA=5*N
506       PRINT*,(VG(I,J),J=NA,NA+4)
          PRINT*,VG(I,10)
          DO 507 N=0,1
          NA=5*N
507       PRINT*,(TG(I,J),J=NA,NA+4)
          PRINT*,TG(I,10)
          DO 508 N=0,5
          NA=5*N+10
508       PRINT*,(UL(I,J),J=NA,NA+4)
          PRINT*,UL(I,40)
          DO 509 N=0,5
          NA=5*N+10
509       PRINT*,(VL(I,J),J=NA,NA+4)
          PRINT*,VL(I,40)
          DO 511 N=0,5
          NA=5*N+10
511       PRINT*,(TL(I,J),J=NA,NA+4)
          PRINT*,TL(I,40)
          DO 510 N=0,5
          NA=5*N
510       PRINT*,(DEL(ID),ID=NA,NA+4)
500       PRINT*,DEL(15)
          GO TO 7
700       PRINT*,((UL(I,J),J=N,15),I=1,2)
          PRINT*,((TL(I,J),J=N,15),I=1,2)
          PRINT*,((UG(I,J),J=1,10),I=1,2)
          PRINT*,((TG(I,J),J=1,10),I=1,2)
7         STOP
C         THIS PROGRAM CANNOT READILY GIVE HEAT TRANSFER COEFFICIENTS
          END
```
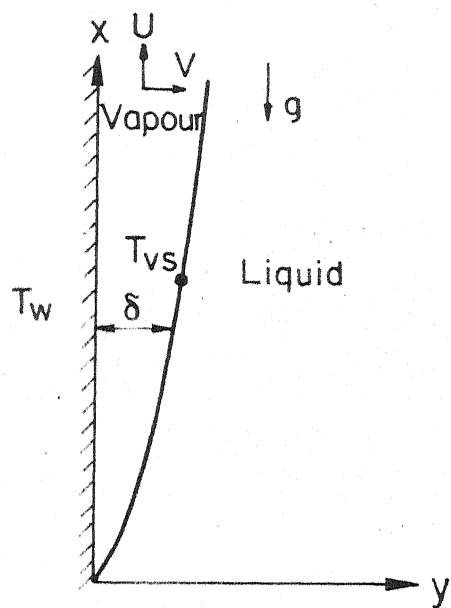
Fig. 2.1 Laminar model
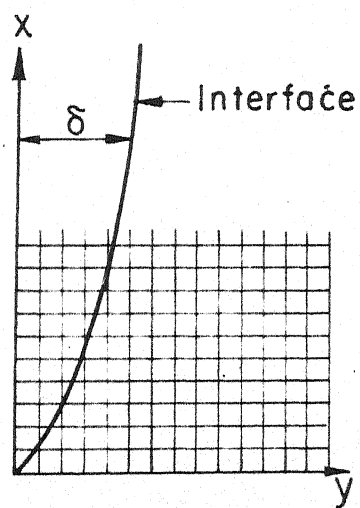
(1)
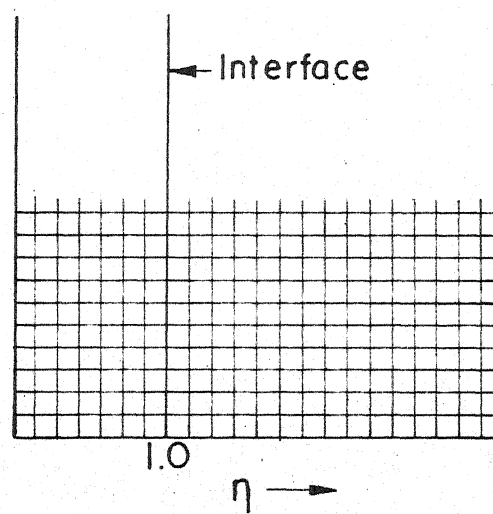
(2)

Fig. 2.2 Grid system
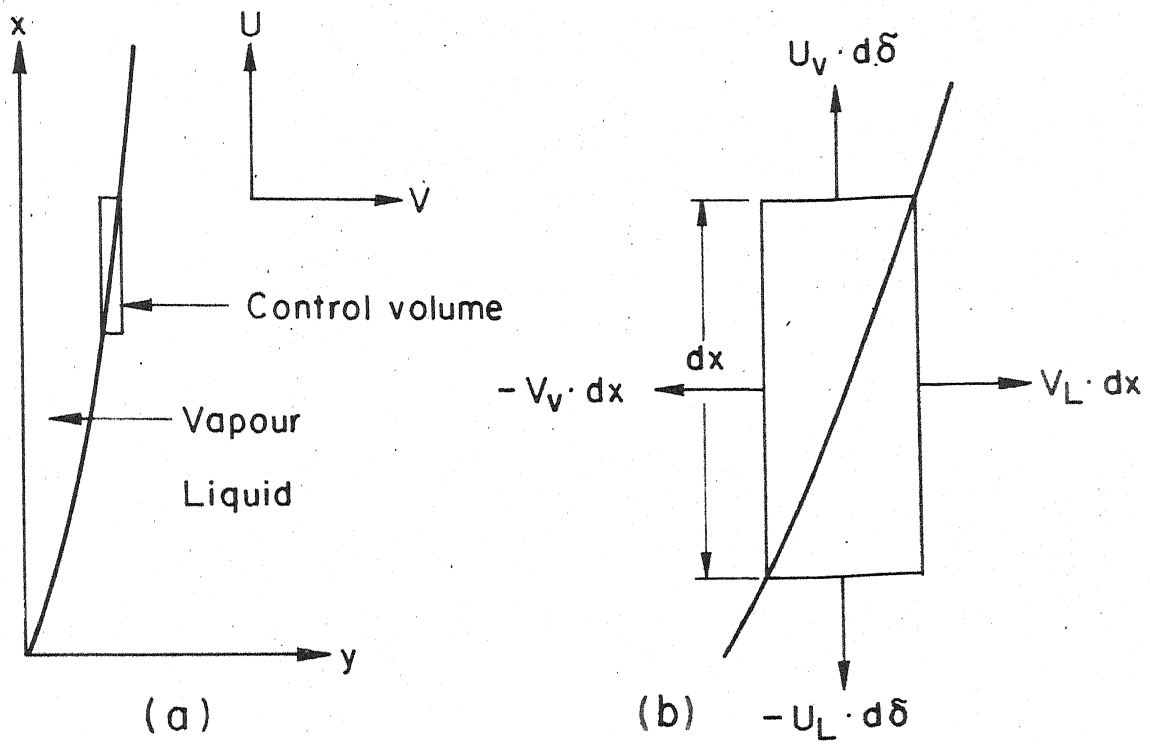
Fig. 2.3   Control volume at the interface
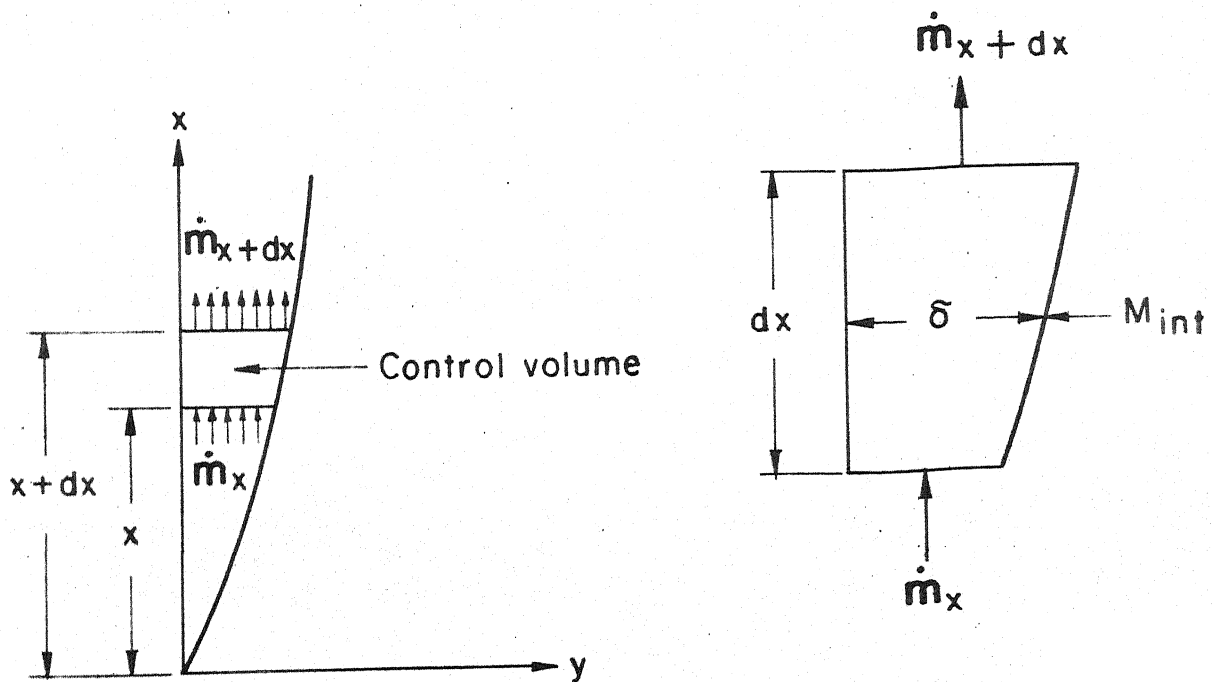
Fig. 2.4   Control volume in vapour region
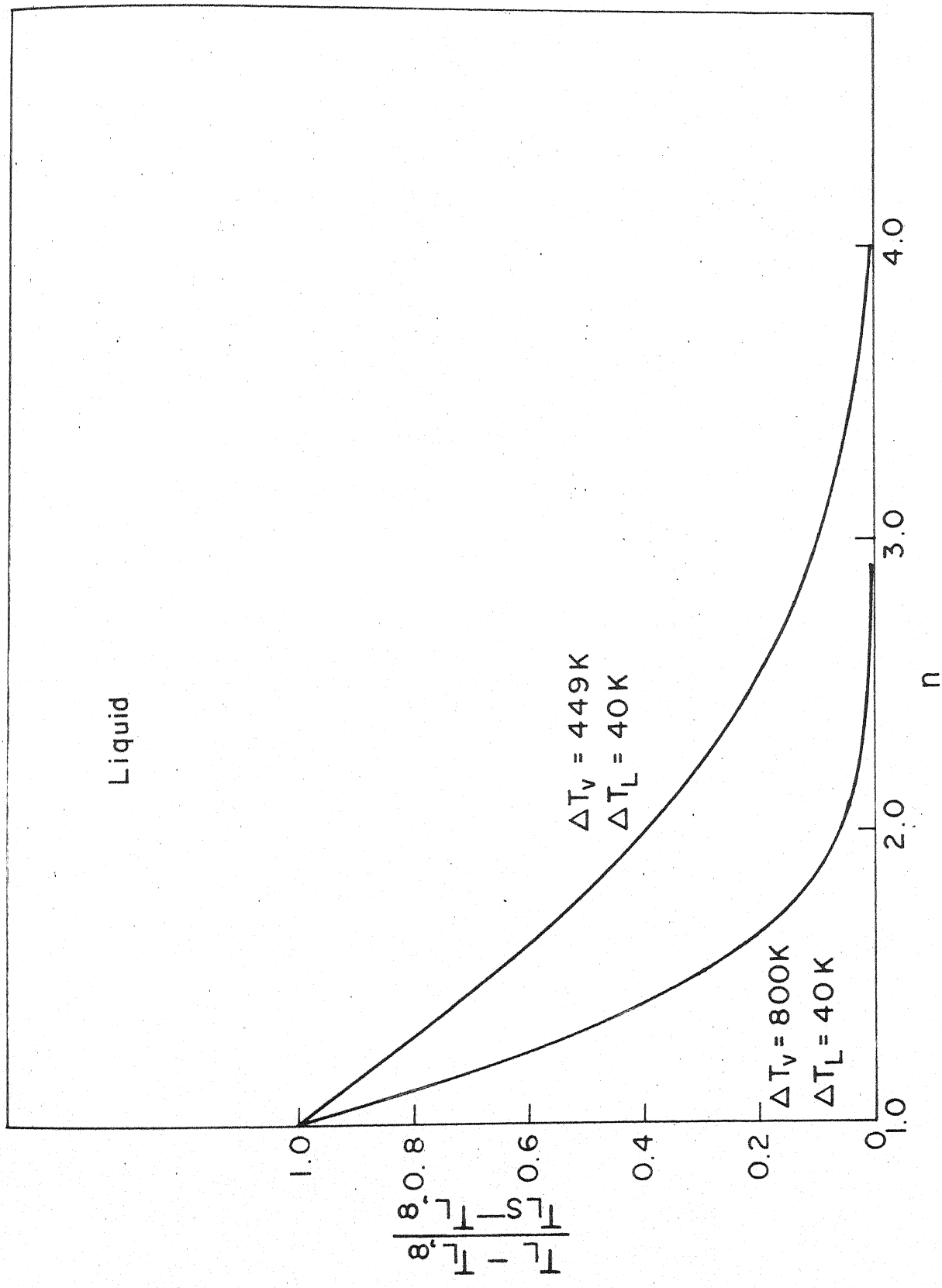
Fig.2.5   Temperature profiles in liquid region
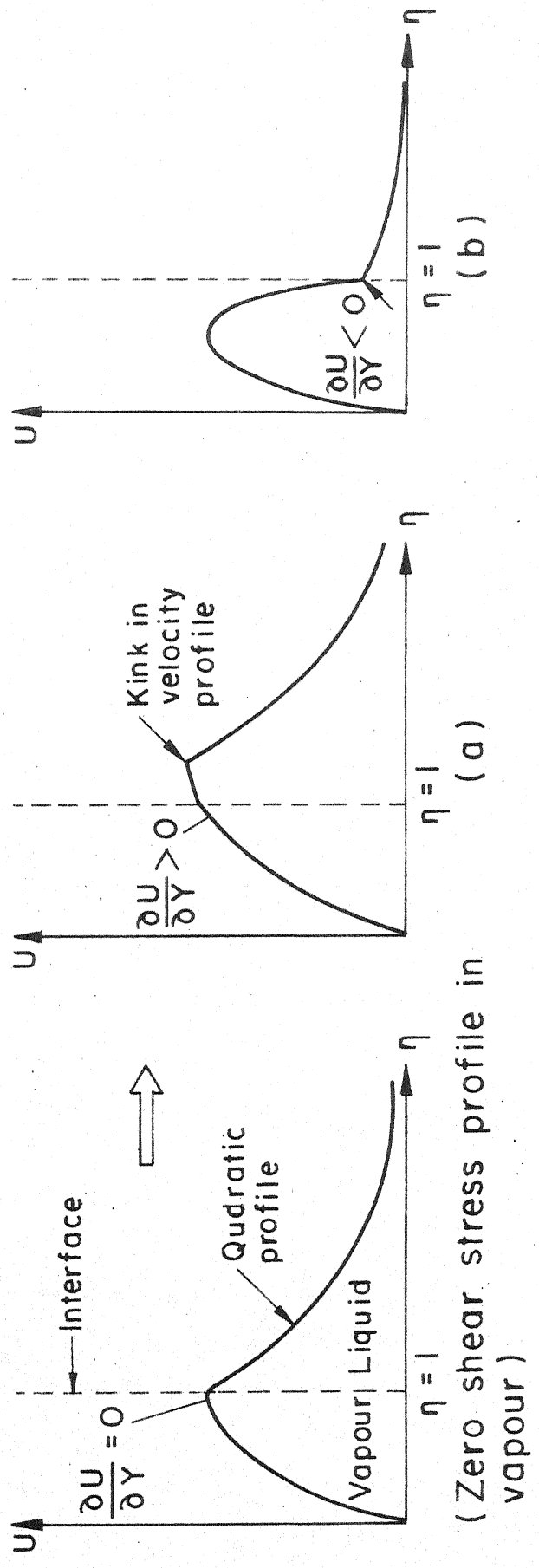
Fig. 3.1 Initial U_v profiles – their possible evolutions
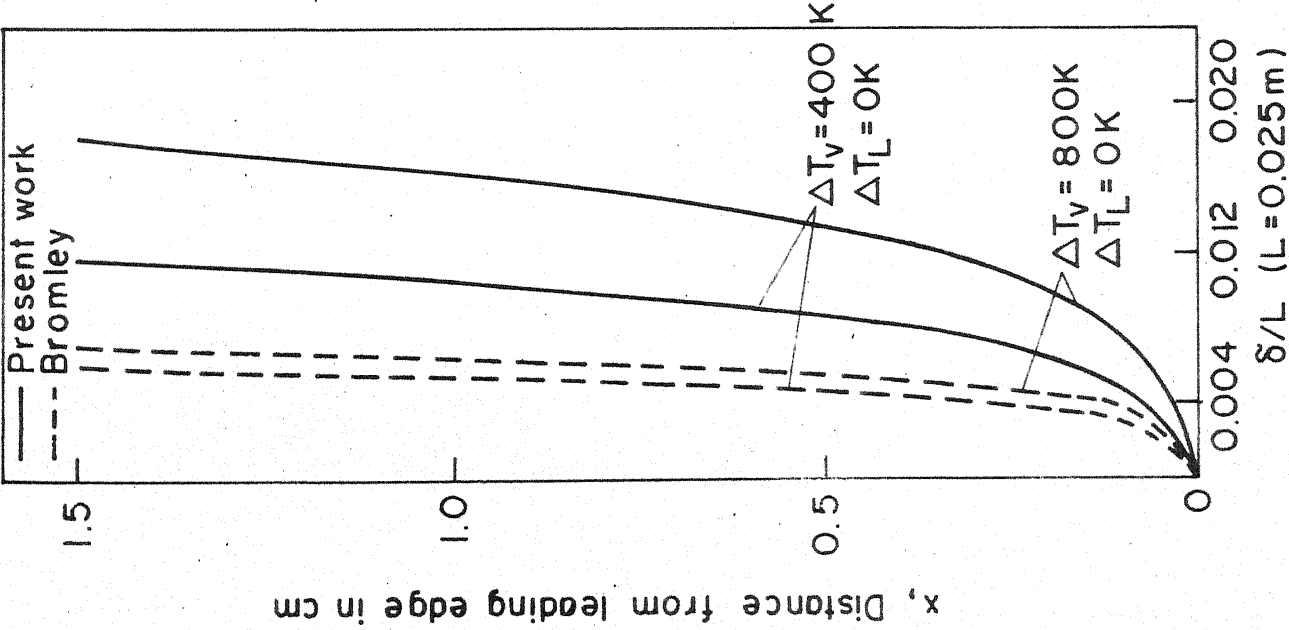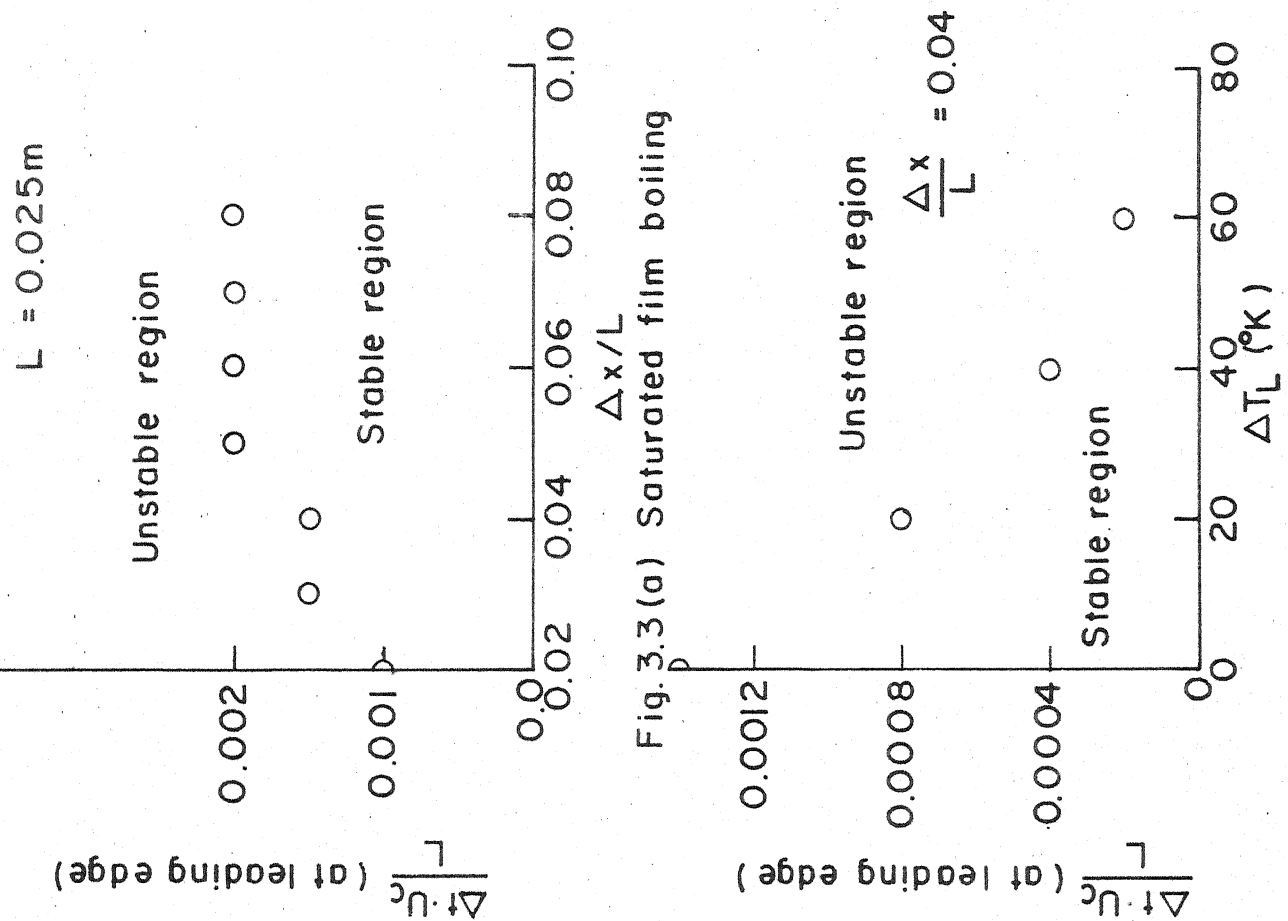
Fig. 3.3(a) Saturated film boiling

$\dfrac{\Delta t \cdot U_c}{L}$ (at leading edge)

L = 0.025m

Unstable region

Stable region

$\Delta x / L$

Fig. 3.3(b) Subcooled film boiling

$\dfrac{\Delta t \cdot U_c}{L}$ (at leading edge)

$\dfrac{\Delta x}{L} = 0.04$

Unstable region

Stable region

ΔT_L (°K)

Fig. 3.2 Variation of boundary layer thickness with x

Present work
Bromley

x, Distance from leading edge in cm

$\Delta T_v = 400$ K
$\Delta T_L = 0$ K

$\Delta T_v = 800$ K
$\Delta T_L = 0$ K

δ/L (L=0.025m)
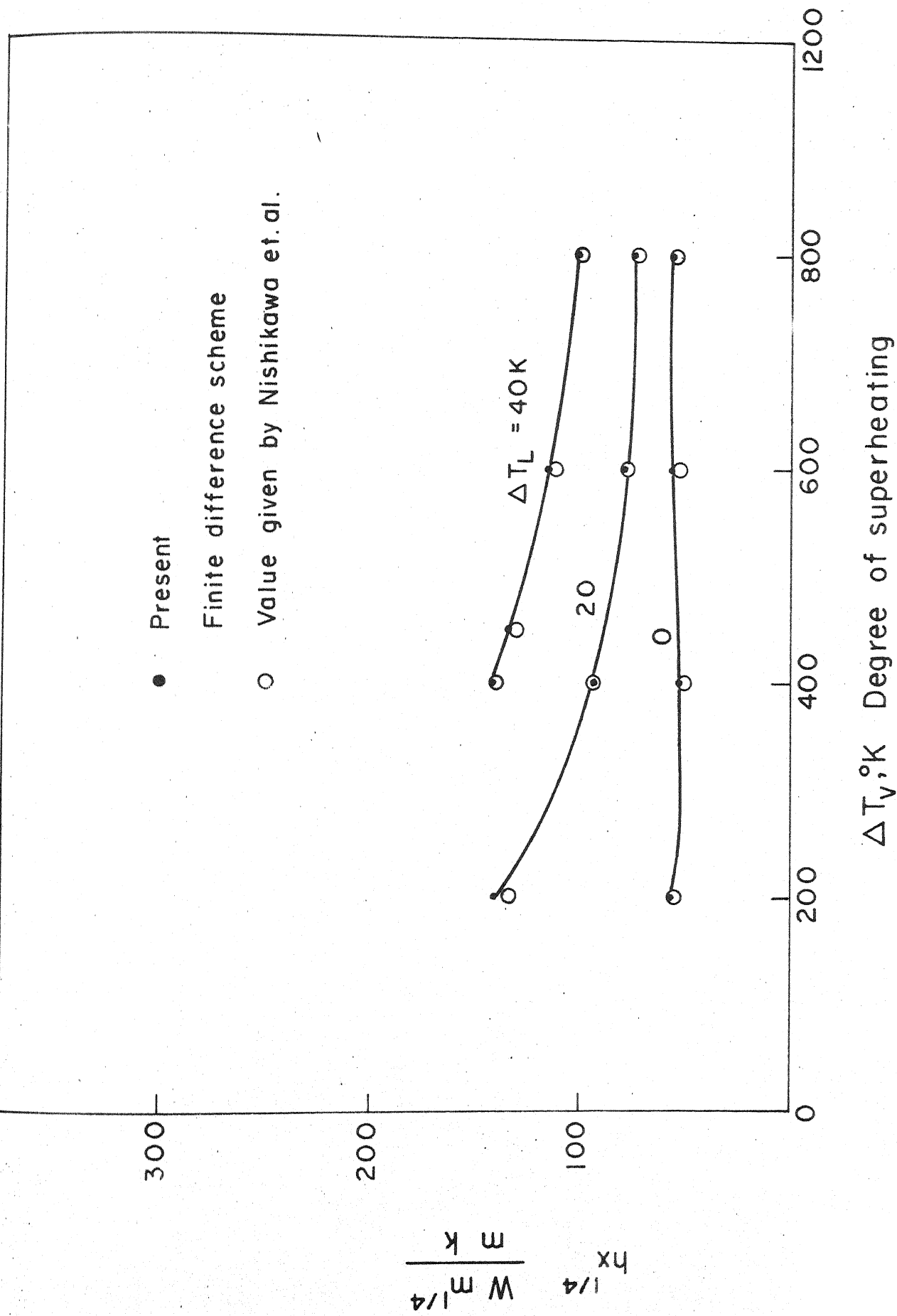
Fig. 4.1 Comparison of heat transfer coefficient with the values given by Nishikawa et. al.
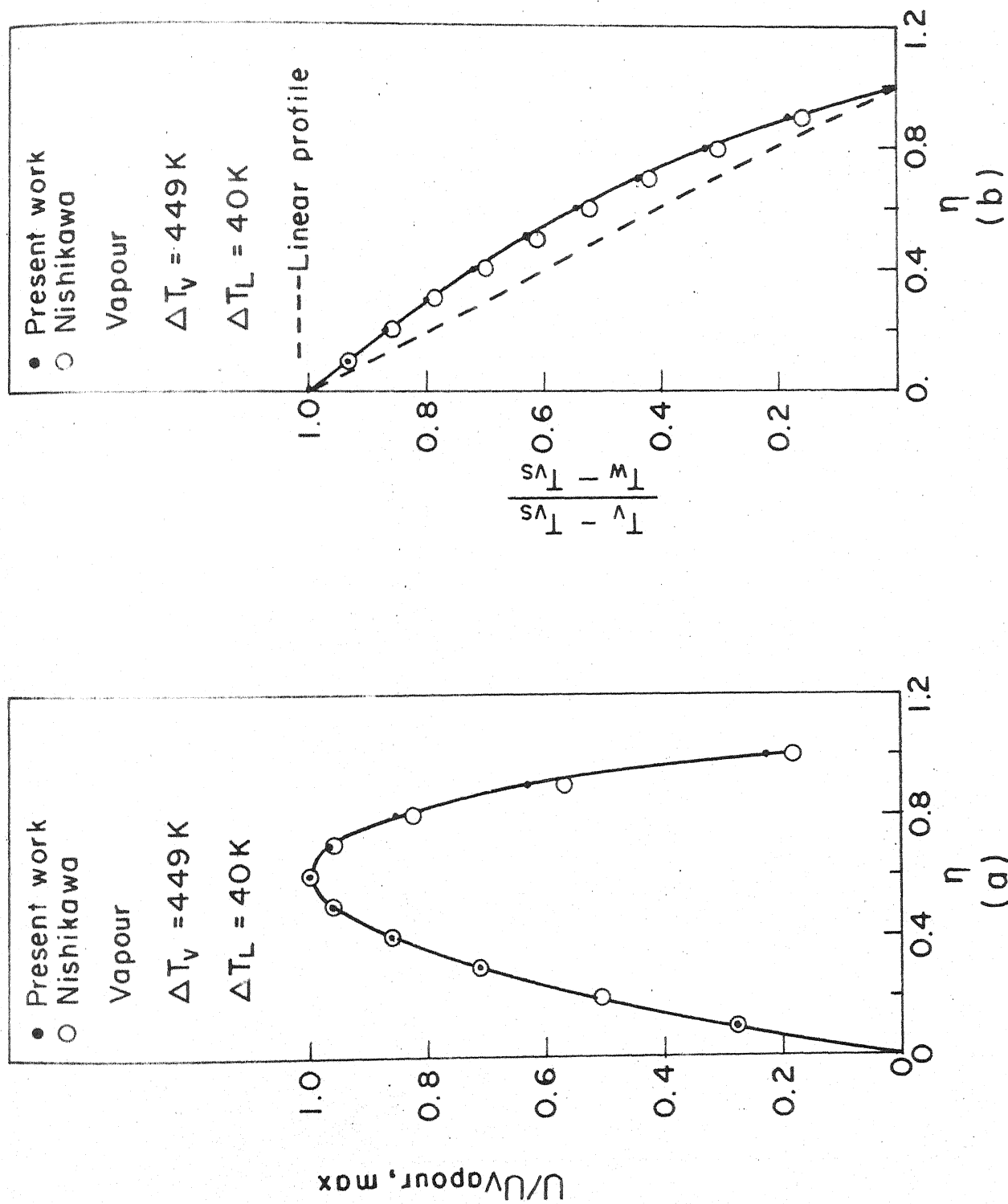
Fig. 4.2 Comparision of velocity and temperature profiles in vapour region
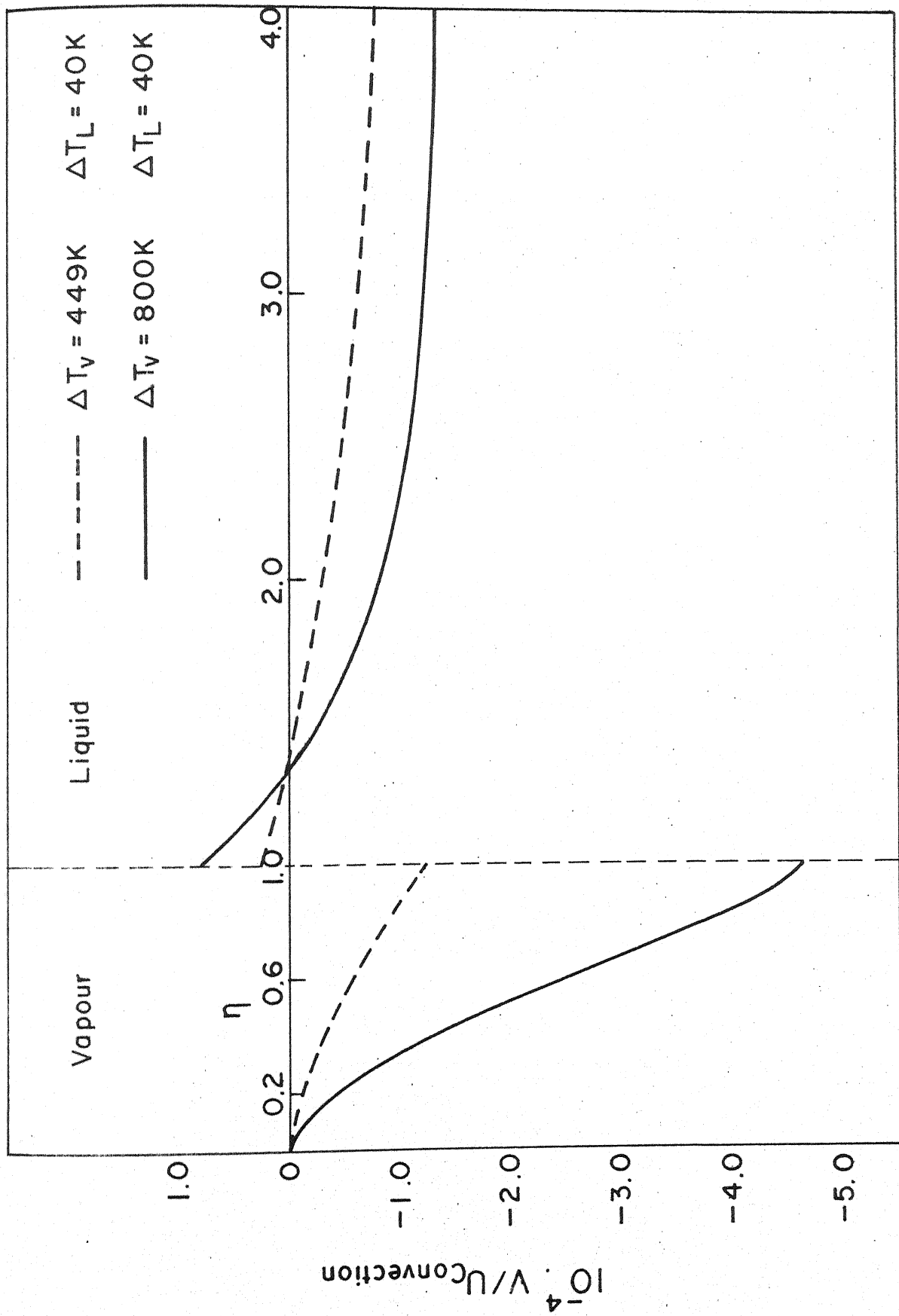
Fig. 4.3   Variation of velocity V with η in vapour and liquid regions
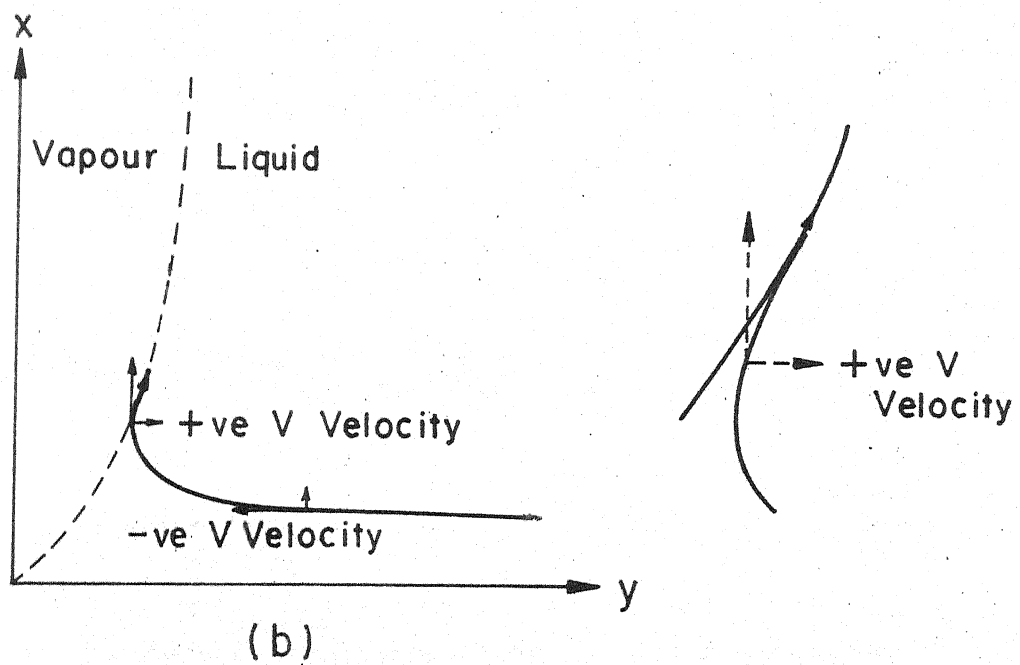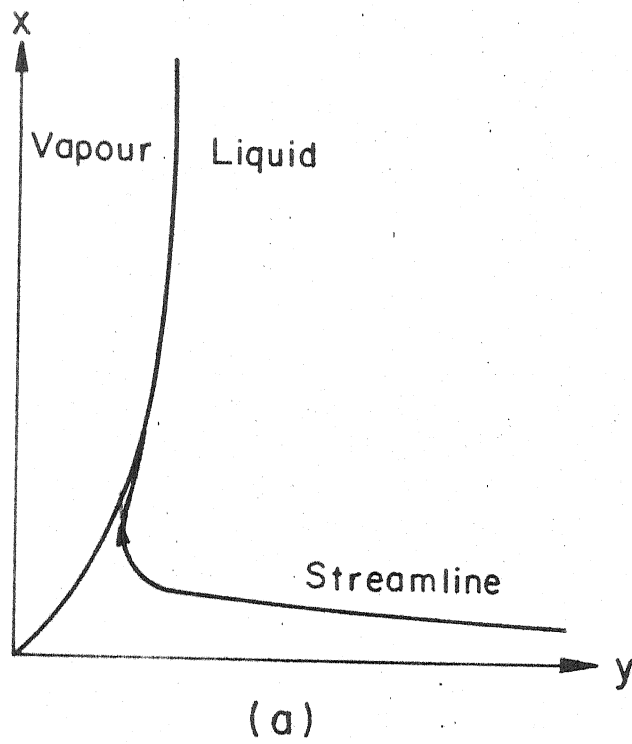
Fig. 4.4 (a, b) Streamline at the interface
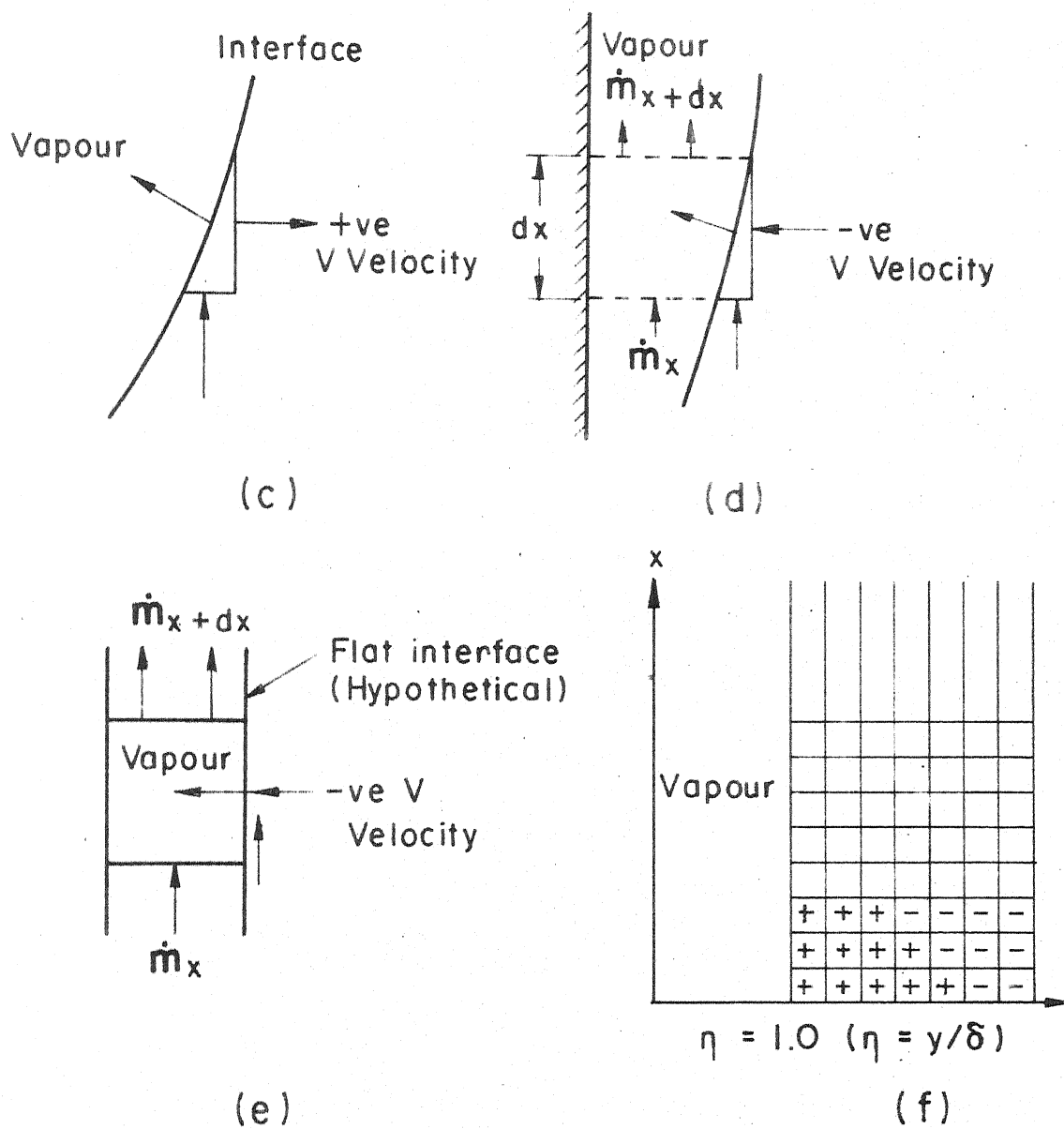
Fig. 4.4 (c,d) Mass conservation at the interface

Fig. 4.4 (e)   Mass conservation for a flat interface
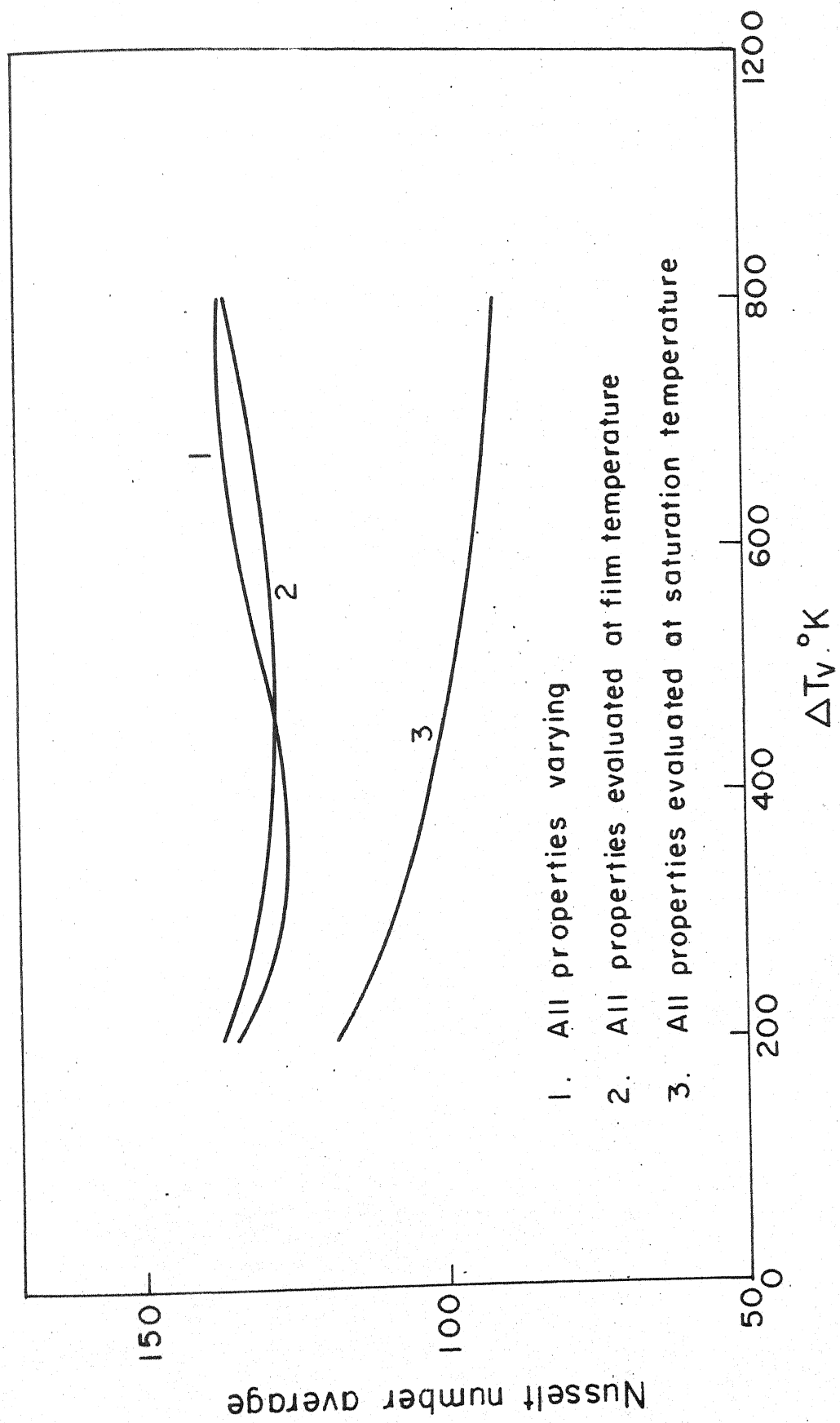
Fig. 4.4 (f)   Sign of V velocity near the interface

Fig. 4.5 Variable property effect on $Nu_{Average}$ in saturated film boiling.
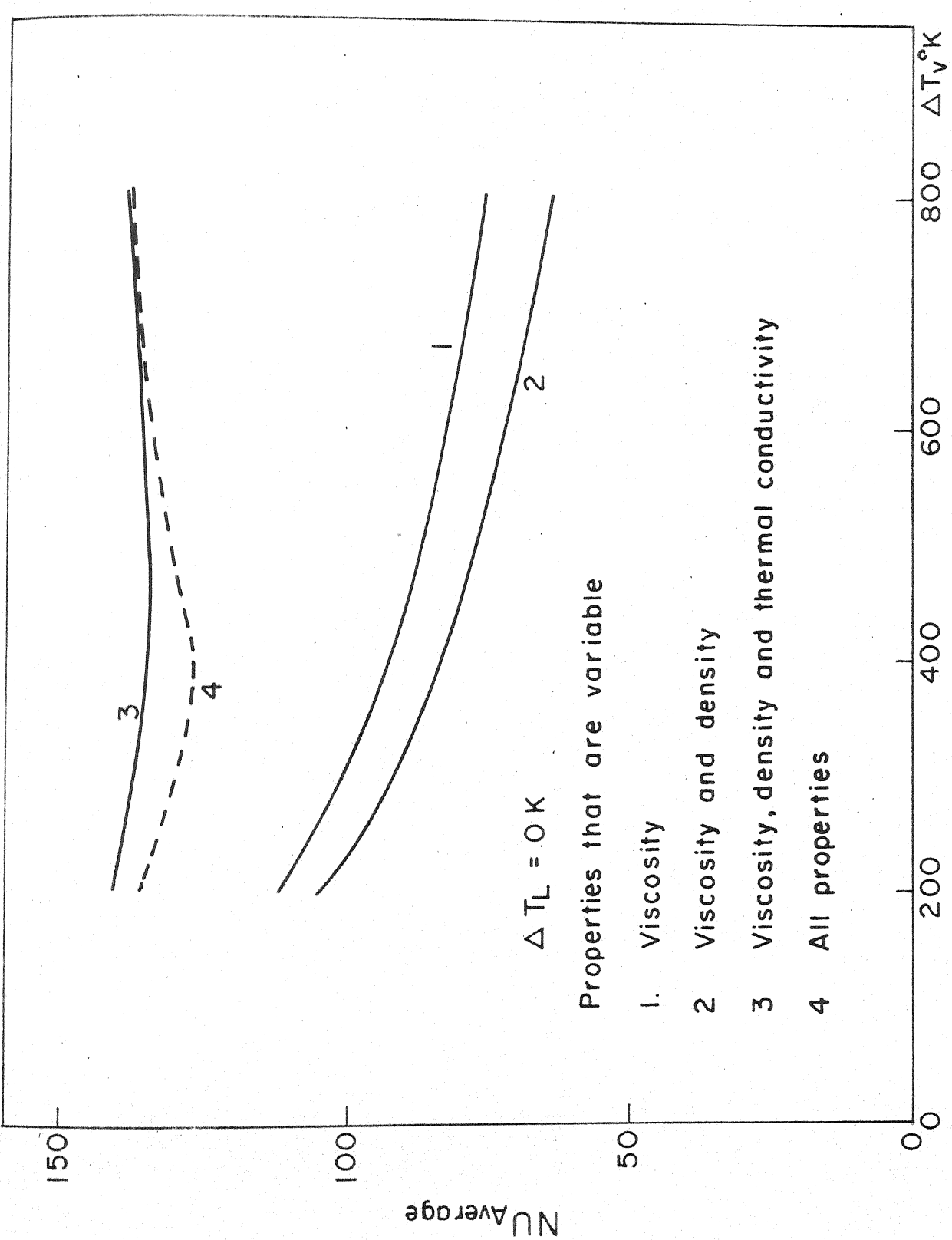
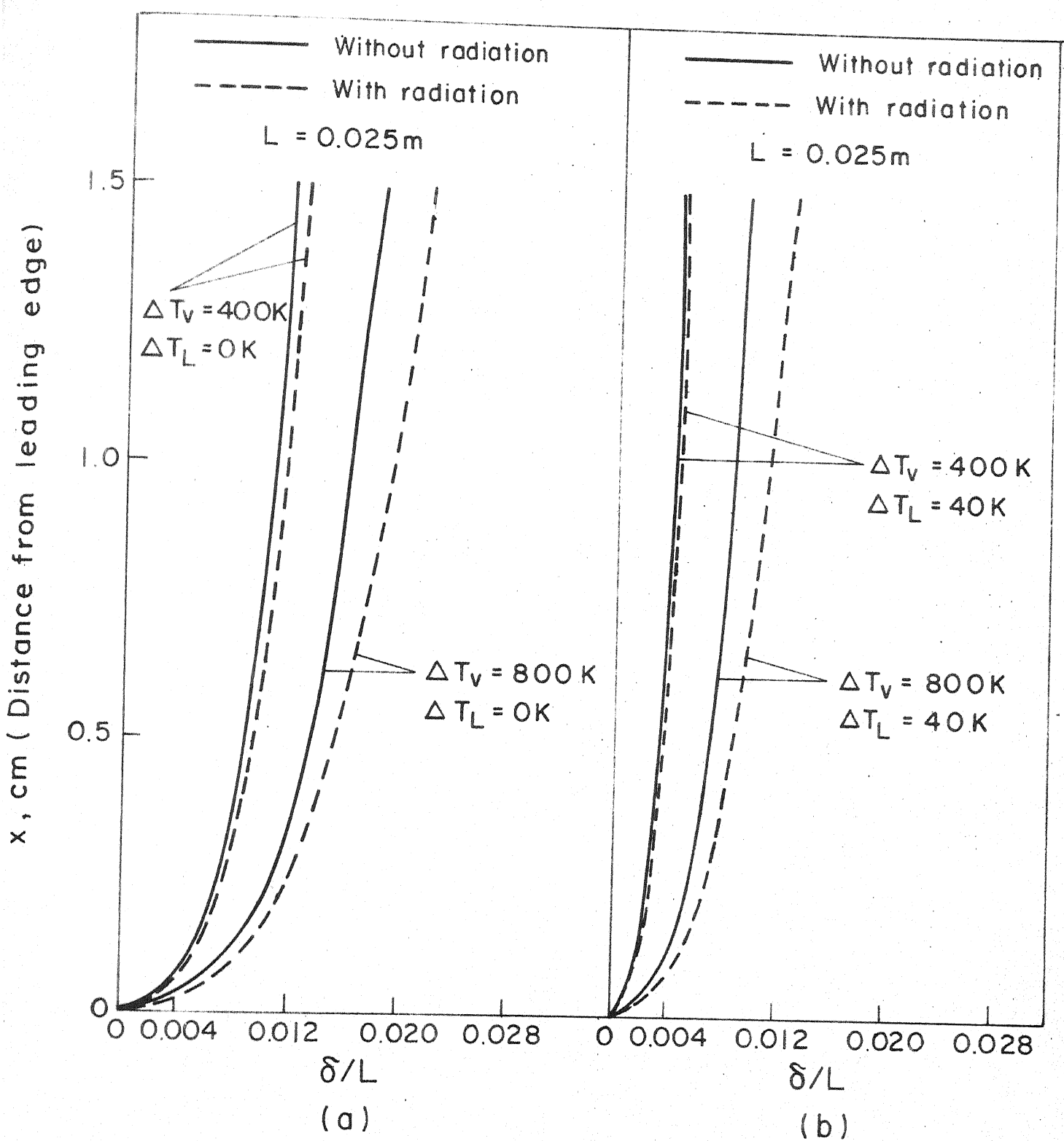Fig. 4.6   Individual effect of properties of vapour on $NU_{Average}$ in saturated film boiling

$\triangle T_L = 0 K$

Properties that are variable

1. Viscosity
2. Viscosity and density
3. Viscosity, density and thermal conductivity
4. All properties

Fig. 4.7 Variation of boundary layer thickness with x
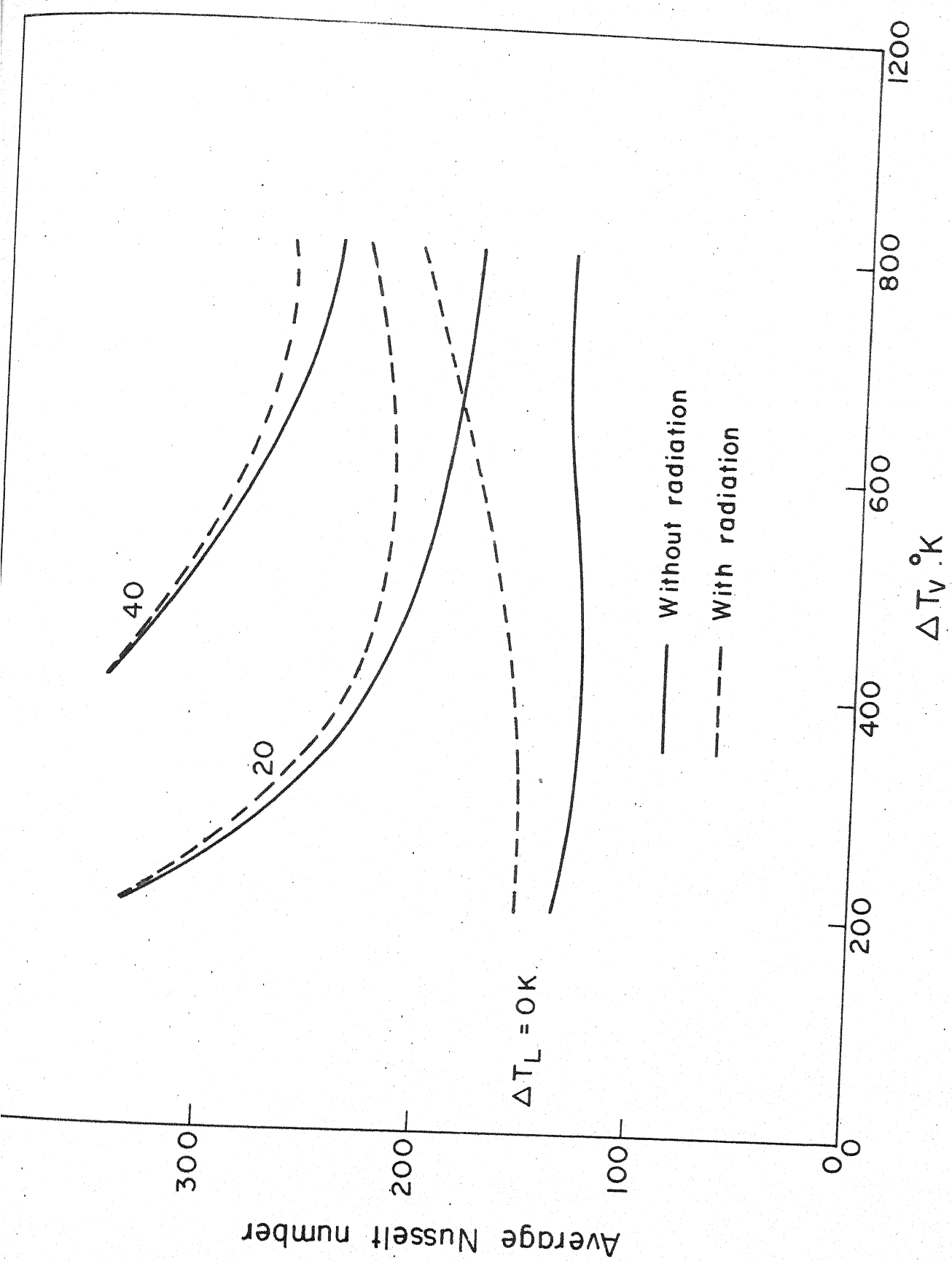
Fig. 4.8 Effect of radiation on $NU_{Average}$

Average Nusselt number

$\Delta T_V \,°K$

$\Delta T_L = 0\,K.$

40

20

—— Without radiation

— — With radiation
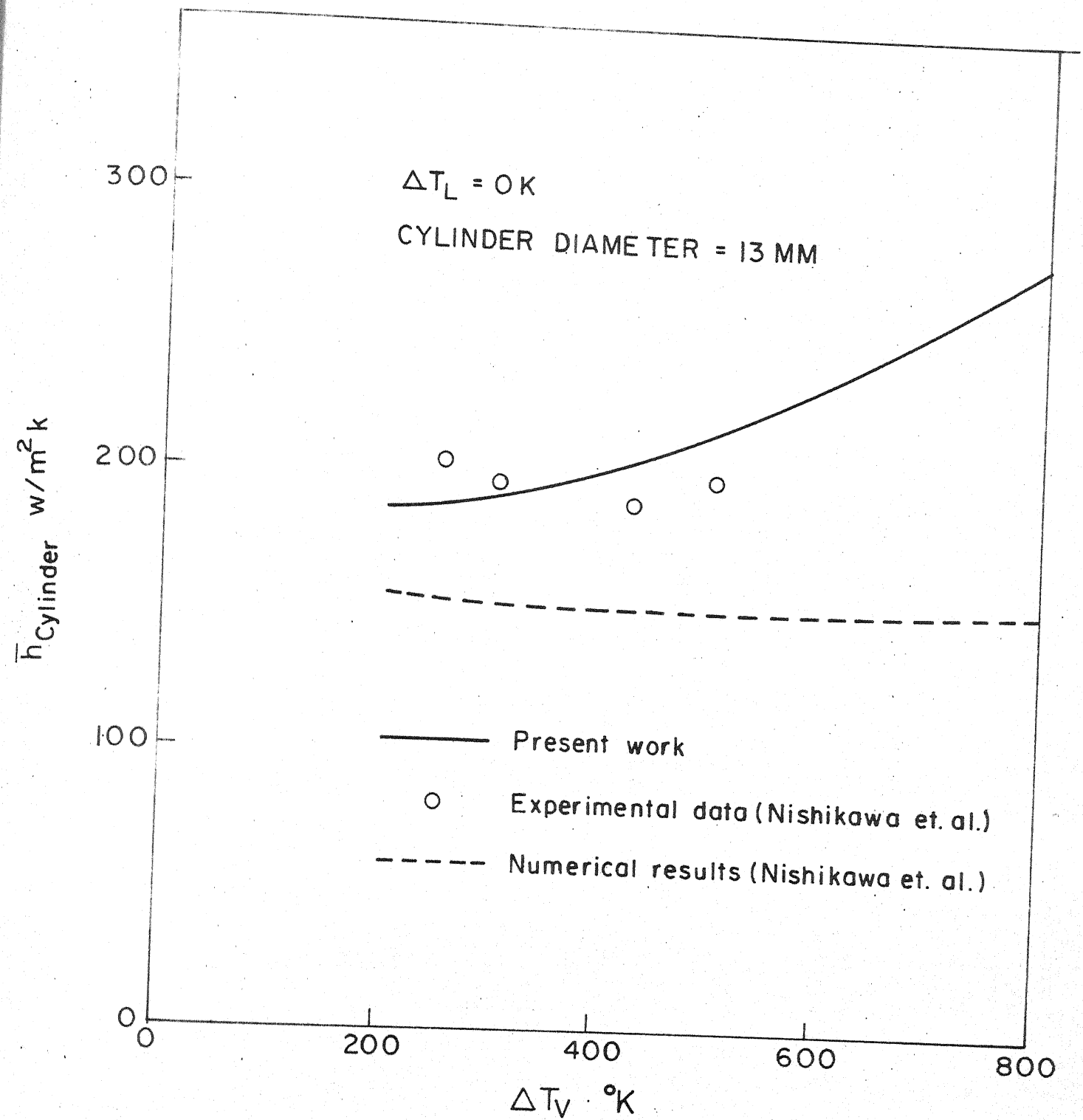
Fig. 4.9 (a)   Verification of present results with experimental data

$\Delta T_L = 0K$

Cylinder diameter = 6mm

—————— Present work

○   Experimental data (Nishikawa)

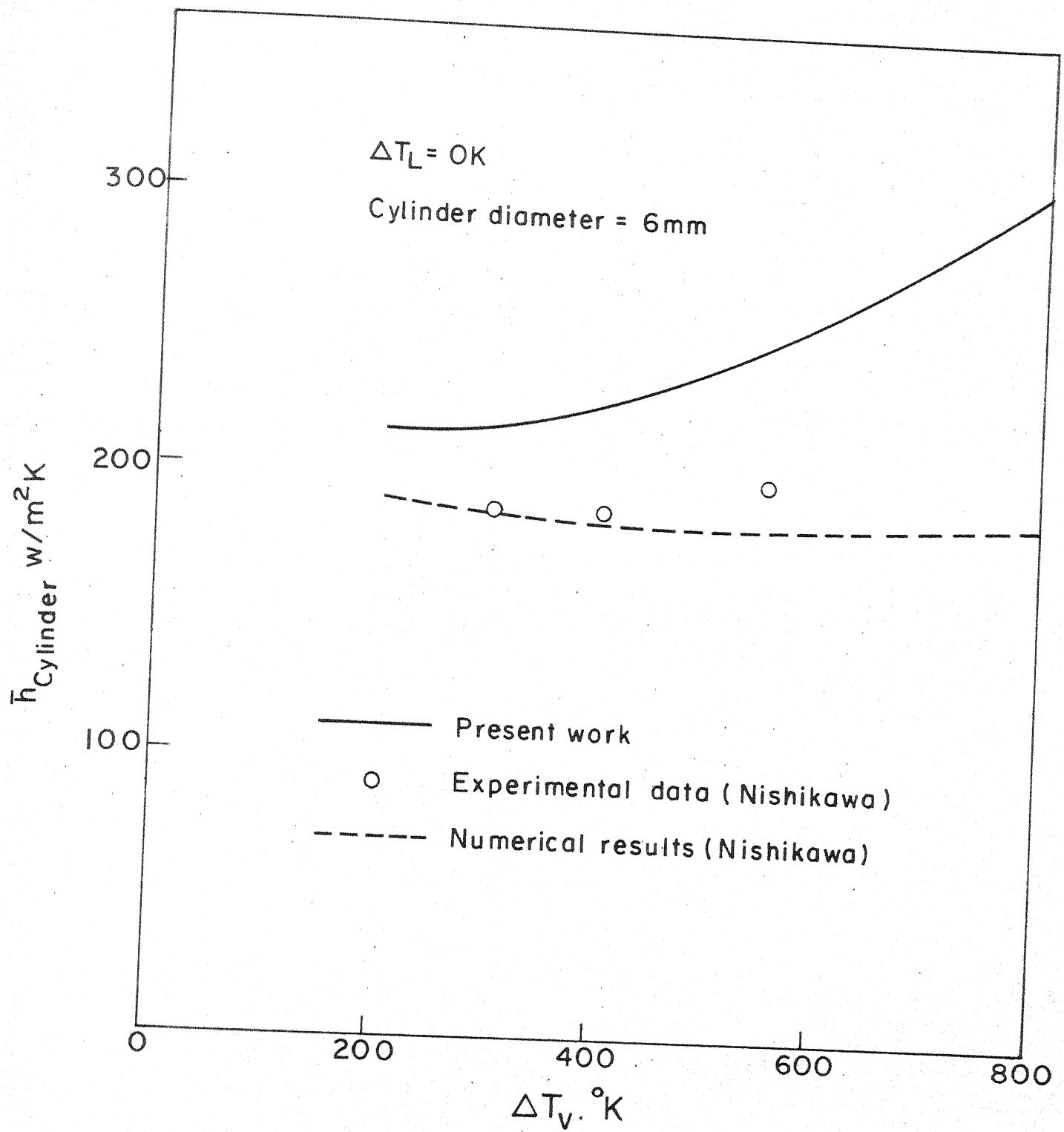– – – – – Numerical results (Nishikawa)

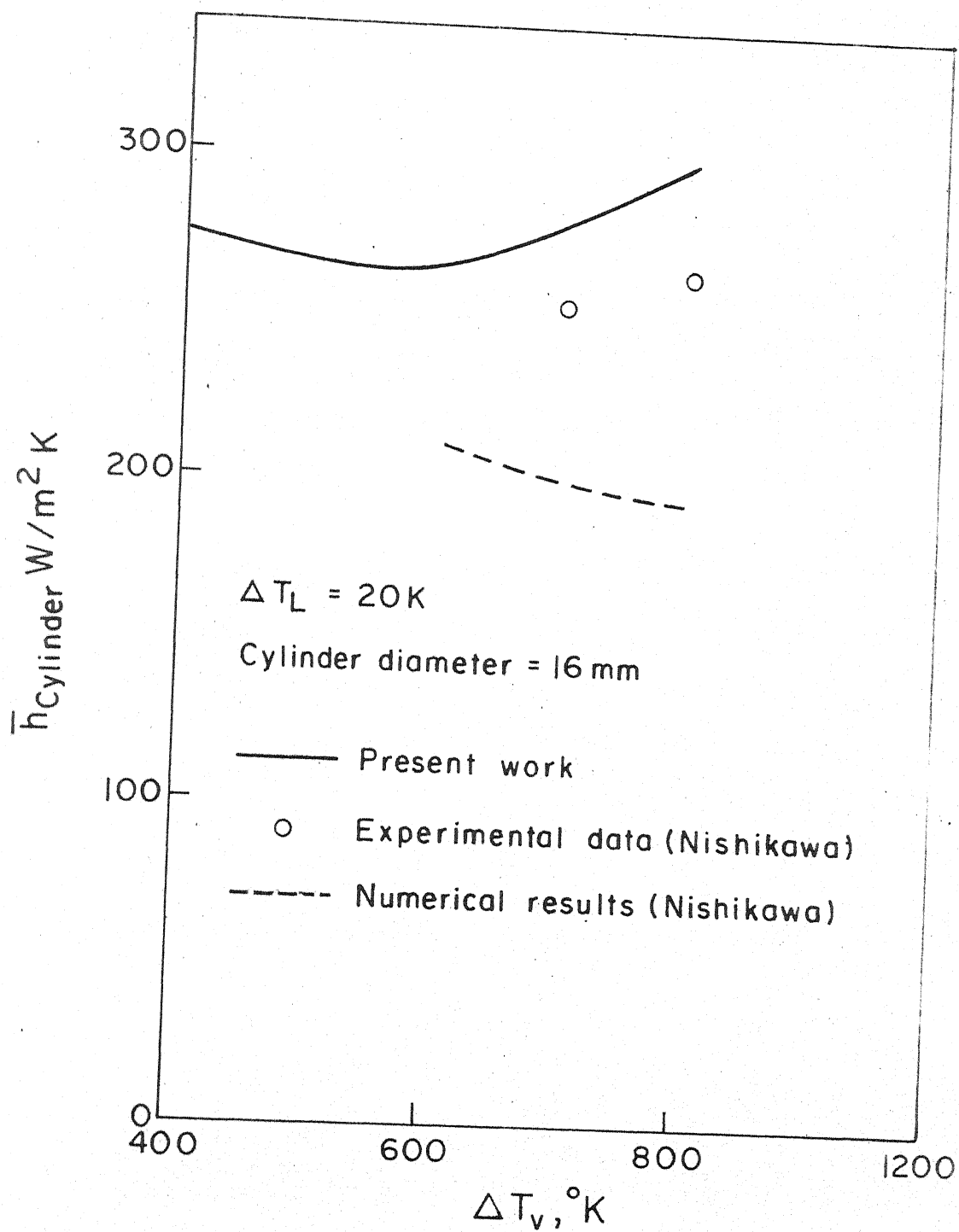Fig.4.9(b)   Verification of present results with experimental data

Fig. 4.9 (c) Verification of present results with experimental data